DISENTANGLING THE NEUROMODULATORY EFFECTS OF TRANSCRANIAL ULTRASONIC STIMULATION OF THE FRONTAL EYE FIELDS IN HUMANS

SOLENN L. Y. WALSTRA

Abstract

Transcranial Ultrasonic Stimulation (TUS) is a novel non-invasive brain stimulation technique that allows modulation of cortical and subcortical brain tissue with unprecedented spatial focality. While online TUS protocols have proven successful in animal studies (Kubanek et al., 2020; Wattiez et al., 2017), evidence in humans remains limited or inadequately controlled (Kop et al., 2023). We therefore aim to establish an effective online TUS protocol for human use with the focus of disentangling excitatory, inhibitory, and perturbatory effects. In this study, we compared the effects of bilateral TUS of the Frontal Eye Fields (FEFs) on saccadic lateralisation in a lateralised choice task, with primary motor cortex (M1) as active control. To enhance methodological validity and reliability, we implemented an auditory mask, control conditions, assessment on efficacy in blinding participants for stimulation conditions, individualised targeting based on functional localisers, and neuronavigation during stimulation sessions. We show that TUS of the left FEF hints at a potential excitatory effect on saccadic direction while TUS of the right FEF hints at a potential perturbatory effect on saccadic accuracy. This hemisphere-specific difference could possibly be due to asymmetry in functional connectivity of the FEFs. However, our small sample size warrants cautious interpretation, precluding definitive conclusions. The present study emphasises control conditions and validated methodology to effectively control confounding factors and disentangle the neuromodulatory effects of TUS in humans.

Supervisors
Assistant Prof dr. Hanneke E.M. den Ouden
PhD candidate Soha Farboud

Affiliation
Radboud University, Nijmegen, The Netherlands
Donders Centre for Cognition, Nijmegen, The Netherlands

Author contact
solennwalstra@hotmail.com

Introduction

Transcranial Ultrasonic Stimulation (TUS) represents a novel non-invasive brain stimulation technique that allows neuromodulation of cortical and subcortical brain tissue with unprecedented spatial specificity (Darmani et al., 2022). This unique featureopens avenues for enhancing causal inference in fundamental intervention studies and exploring potential clinical applications. While animal studieshave demonstrated the efficacy of online TUS protocols in modulating behaviourduring or immediately after stimulation (Kubanek et al. 2020; Wattiez et al., 2017),evidence in humans remains limitedor inadequately controlled (Kop et al., 2023). Given the foundational stage of TUS in humans, there is a criticalneed to develop protocols that maximise efficacy while minimising confounding factors. This approach ensures unequivocal inference from behavioural modulation and offers insights into the neuromodulatory effects of TUS.

TUS operates by emitting low-intensity ultrasonic waves beyond human hearing range through the scalp and skull, enabling non-invasive neuromodulation of brain regions (Blackmore et al., 2019; Darmani et al., 2020). The acoustic mechanism allows interaction with neuronal tissue, providing millimetre-level spatial specificity even in deep-seated brain regions. These unparalleled spatial features in targeting are facilitated by TUS' reducedattenuation of mechanical vibrations passing throughthe skull, resulting in diminished scattering and dispersion within neuronal tissues. As a result, TUS thereby overcomes the trade-off between depth and accuracy inherent in traditional non-invasive brain stimulation methods such as Transcranial Magnetic Stimulation (TMS) and Transcranial Electrical Current Stimulation (tES). Previous studies have leveraged this unique opportunity, demonstrating the efficacy of TUS in modulating behaviour (animals: Folloni et al., 2019; Fouragnan et al., 2019; Khalighinejad et al., 2020; Pouget et al., 2020; humans: Butler et al., 2022; Nakajima et al., 2022), gamma-aminobutyric acid (GABA)/glutamate (Glu) balance (animals: Yang et al., 2012; humans: Yakuub et al., 2023), and functional connectivity (animals: Folloni et al., 2019; Khalighinejad et al., 2020; Verhagen et al., 2019; humans: Ai et al., 2016; Badran et al., 2020), resulting in diverse outcomes including excitatory, inhibitory, or perturbatory effects. However, most of these studies have employed offline paradigms, focusing on enduring aftereffects of TUS. While offline protocols hold promise for clinical applications, online protocols are essential for a deeper understanding of neuralmechanisms with greatertemporal precision.

Despite the potential of online TUS protocols in humans, evidence supporting their efficacy while minimising confounding factors remain scarce.To accurately assess the efficacy of a neuromodulation protocol, a clear definition of the fundamental components is essential. This includes establishing a distinct brain- behaviour relationship (Darmani et al., 2022), exemplified by the interaction of the cortical region Frontal Eye Field (FEF) with eye movements. The FEFs are pivotal in representing visual stimuliin the contralateral visual hemifield and controlling contralateral voluntary eye movements, such as saccades(Beurze et al., 2009; Curtis& Connolly, 2008; Paus, 1996).

The functional lateralisation in oculomotor controlinvolves increased activityin FEFs neuronsin one hemisphere when theirreceptive fields containa task-relevant target,controlling saccades towardsthe contralateral visualhemifield (Schall & Hanes, 1993; Schall et al., 1995). Conversely, FEF neurons in the ipsilateral hemisphere, with task-irrelevant targets in their receptive fields, are inhibited. This dichotomy in FEF neural activity is believed to be facilitated by interhemisphericinhibitory connections (Schlag et al., 1998). Moreover,excitation induced by (non-
)invasive stimulation, predominantly influences contralateral eye movements, while inhibition caused by unilateral lesions or (non-)invasive stimulation, primarily affects ipsilateral eye movements (for a comprehensive review, refer to Vernet et al., 2014). Importantly, this relationship between neural activity and behaviour remains consistent across species. Specifically, animal studies have shown that neuronal activity in the FEFs gradually increasesduring stimulus presentation, correlating with accumulation of evidence for one of the choice options. This activity governs the generation and control of saccades (Ding & Gold, 2012; Hanks et al., 2015; Kayser et al., 2010). This notion is reinforced by Murd and colleagues (2020), who found that TMS delivered to the human FEFs affected performance in a perceptual decision-making task. Notably, this effect was observed only when TMS was delivered during information integration, rather than during subsequent categorical choice. These findings suggest a reliance of the human FEFs on the gradual accumulation of information that provides evidencein favour of one of the choice options, known as evidence accumulation in decision-making (Bogacz et al., 2006; Hanks et al., 2015). Revisiting our initial premise, the high-fidelity readout of lateralised FEF neural activity in lateralised saccadic direction, combined with precise measurements provided by an eye tracker, equipped us with a robust foundation to accurately assessthe efficacy of an onlineTUS protocol.

In this endeavour, we adopted a well-established online TUS protocol that target the FEFs in non-human primates by Kubanek et al. (2020), in conjunction with a choice task as focal point. Their study demonstrated biased saccadic eye movements after lateralised TUS of the FEFs during a two-alternative forced choice (2AFC) perceptual decision-making task, showcasing excitatory TUS effects. In this task, subjects are instructed to execute saccades towards the first of two consecutively appearing targets in each hemifield, with varying target onset delays. These varying delays inherently facilitate the gradual accumulation of evidence, thereby shaping the choice-making process for each saccadic direction. Longer target onset delays encourage early and robust evidence accumulation favouring one saccadic direction over the other, often resulting in reflexive saccades to the first target. Conversely, shorter target onset delays would provide less robust information which target appeared first, leading to slower evidence accumulation and creating a near-equilibrium between the two saccadic directions. In this latter scenario, the uncertainty requires top-down inhibition where reflexive saccades to the second target need to be suppressed and voluntary saccades towards the first target need to be facilitated. Interestingly, incorporating TUS during the 2AFC saccade task would introduce a new dimension. While its influence may be negligible during longer target onset delays, where evidence accumulates early and robustly, TUS may become pivotal during shorter target onset delays characterised by uncertainty in accumulating evidence. In such cases, TUS has the potential to bias saccadic direction.

Although our measurements primarilyfocus on behavioural outcomes, the observed effects at this higher-order cognitive level in fact originate from the intricate interplaybetween TUS and neuronal tissue.However, the specific biomechanism underlying TUS effects remains unclear. Studies have proposed various biomechanisms. TUS may directlyor indirectly open mechanosensitive ion channels at various locations, allowing influx and outflux of calcium or sodium ions, which lead to excitatory effects, while the outflux of potassium ions results in inhibitory effects (Sorum et al., 2021; Yoo et al., 2022). Alternatively, TUS may induce pressure changes in the cell membrane,altering the thresholds of excitatory or inhibitory postsynaptic potentials, and thereby impacting action potentials (Jerusalem et al., 2019; Yoo et al., 2022). Considering the intricate nature of neural circuits and networks in addition to region-specific modulation, it is highly likely that multiple mechanisms are at play. As a result, a combination of these mechanisms could lead to perturbatory effects, especially at the behavioural level.

Our study investigated the direct neuromodulatory effects of TUS on behaviour, with a focus on disentangling between excitatory, inhibitory, and perturbatory effects. We hypothesised that TUS of the FEFs may introduce a bias in saccadic direction during shortertarget onset delays.Given the lateralised relationship between neural activity and behaviour, this bias could either enhanceevidence accumulation for the contralateral saccadic direction, thereby increasing the probability of choosing the contralateral target—indicative of an excitatory effect (Figure 1A). Conversely, it could diminish accumulation of evidence for the contralateral saccadic direction, leading to a decreased probability of choosing the contralateral targetand relatively favouring the target in the ipsilateral hemifield—indicating an inhibitory effect (Figure 1B). Alternatively, TUS might distort the balance of evidence, narrowing the gap of evidence between the two targets and potentially decrease saccadic accuracy—generating a perturbatory effect (Figure 1C). Altogether, the robust relationship betweenneural excitation, inhibition, and perturbation within the FEFs, along with the direct behavioural read-out of the FEFs, ensures that any behavioural changesresulting from the interaction of TUS with neuronal tissue can be unequivocally attributed to the corresponding neuromodulatory effects.This not only facilitates assessment of the protocol's efficacybut also providesprecise insights into the natureof the TUS neuromodulatory effects.

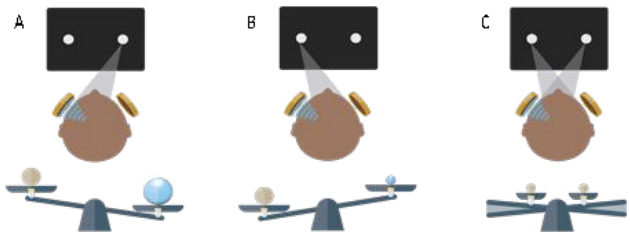

Figure 1 | Hypothesised neuromodulatory effects of TUS of the FEFs on evidence accumulation and saccadic direction given shorter target onset delays. (A) Enhanced evidence by TUS for target in contralateral hemifield (increased blue sphere) would yield increased contralateral saccades, indicative of an excitatory effect. (B) Diminished evidence by TUS for targetin contralateral hemifield (decreased blue sphere) would yield increased ipsilateral saccades, indicative of an inhibitory effect. (C) Distorted evidence by TUS for both targets (uncertainty) would yield increased saccades randomness such as decreased saccadicaccuracy, indicative of a perturbatory effect.

Importantly, maximising the protocol's efficacy is intrinsically liked to minimise confounding factors, as both are essential for clear insights into the neuromodulatoryeffects. To minimise confounds, we implemented several methodological considerations. Given the high spatial specificity of TUS and the inter-individual differences in brain morphology, along with variability in localisation of the human FEFs acrossstudies (Amiez et al., 2006, 2009; Gagnon et al., 2002; Ionnaides et al., 2010; Paus, 1996; Vernet et al., 2014), we utilised an MRI-based functional localiser to obtain the stimulation coordinates for each participant. Neuronavigation guided precisetargeting throughout the stimulation sessions. Additionally, a recent multicentre study has identified challenges associated with somatosensory and auditory confounds in online TUS protocols (Kop et al., 2023). Thus, our stimulation sessions were double-blind, incorporating sham stimulation and an active control region. The active control involved stimulating the primarymotor cortex (M1; hand area)—asimilarly located motorbrain region—to controlfor somatosensory effects, in addition to the mutual control within the FEFs. To account for putative auditory confounding factors, an auditory mask was employed to blind participants for various stimulation conditions, with a separate assessment conducted to verify its effectiveness. With these methodological considerations in place, our approach enables assessment of the protocol's efficacy, provides insights into the neuromodulatory effects, and facilitate disentanglement betweenexcitatory, inhibitory, and perturbatory effects.
Taken together, this study paves the way for future investigations endeavours seekingto refine TUS protocols in humans, deepenour comprehension of the associated neuromodulatory effects, and explore their potential applications in deeper brain regions linkedto clinical disorders.

Methods

Participants

Currently, we have successfully recruited eight individuals who have completed all three parts of the study (Mage = 27, SDage = 3.50, age range 21-33, seven female). We aimto collect data from a total of 36 healthy right-handed participants aged between 18 and 40 years. The estimated effect size for the power analysis was determined by reference to previous TUS studies involving behavioural modulation (Fomenko et al., 2020; Legon et al., 2014, 2018; Liu et al., 2021). The chosen effect size, falling within the small to medium range (f ~ .35), was selected at an alpha level of .05 with a desiredpower of 80% (G*Power 3.1, Faul et al., 2009).Exclusion criteria consisted of a historyof brain surgery,serious head trauma, epilepsy, convulsion or seizure, the presence of implanted metal in the head or upper body, diagnosedneurological or psychiatric disorders, and consumption of either more than four alcoholic units within the preceding 24 hours or any recreational drugs within the past 48 hours. Written informed consent was obtained from all participants accordingto the Declaration of Helsinki.The experimental procedures were approved by the Medical Research Ethics Committee (proposal no. NL76920.091.21).

Study design

This pre-registered study consisted of three parts: an intake session and two double-blind, within-subject, sham-controlled TUS sessions(Farboud et al., 2023; Figure 2A). The two TUS session were spaced approximately one week apart, with intervals of up to three months between sessions, all scheduled at consistent times of the day to control for metabolic fluctuations.

During the intake session,participants first engagedin a 15-minute practice of the saccade task without TUS delivery. Following this, they entered the MRI scanner to acquire structural scans (T1-weighted, T2-weighted, and UTE) for neuro navigation and acoustic and thermal simulations, respectively—of which the latter two scans will be utilised for the complete study in future. Additionally, participants performed FEF and M1 functionallocalisers, crucial for obtaining stimulation coordinates. Finally, GABA/Glu ratios were acquired from the stimulation regions in the left hemisphere using single voxel magnetic resonance spectroscopy (MRS), with only GABA baseline levels explored for the presentstudy (referto Supplemental materials). During the two subsequent brain stimulation sessions, participants performed the saccade task whilst receiving a pseudo randomised sequence of TUS (TUS of the left and rightFEF and M1) and sham. There were two TUS-block sequences with a specific orderof the FEF-blocks and M1-blocks. Participants completed both sequences, randomised and counterbalanced across the two stimulation sessions (Figure 2B). Each stimulation session began with screening and a 45-minutepreparation phase (referto Preparation and neuro navigation section). Once preparations were completed, participants firstly performed a practice block of the saccade task—without TUS delivery or auditory masking—to reacquaint themselves with the task. Performance below 60% of the maximum score triggered an automatic repetition of the practice block. After practice,the saccade task with TUS delivery commenced,with the corresponding sequence of FEF-blocks and M1-blocks. Preceding and succeeding each TUS block, a baseline block without TUS delivery or auditory masking occurred. TUS blocks contained three conditions: i) left TUS, ii) right TUS, and iii) sham, all with an auditory mask. The order of conditions within TUS blocks followed a pseudo random pattern limited to a maximum of four consecutive trials of the same condition, while all conditions are equally represented.

The stimulation sessions were conducted in a double-blind manner to compare TUS administered on the left and right sides, as well as active stimulation versus sham, ensuringthat neither the experimenters nor the participants were aware of the stimulation conditions within each block. However,the stimulations sessions were single- blind with respect to the block type of FEF or M1, as experimenters positioned the two TUS transducers based on the corresponding TUS-block sequence.

At the end of each stimulation session, participants were queried about any symptoms they believed could be associated with TUS. Only after the second stimulation session, an assessment of auditory masking was conducted to evaluate the effectiveness of blinding participants to various stimulation conditions.

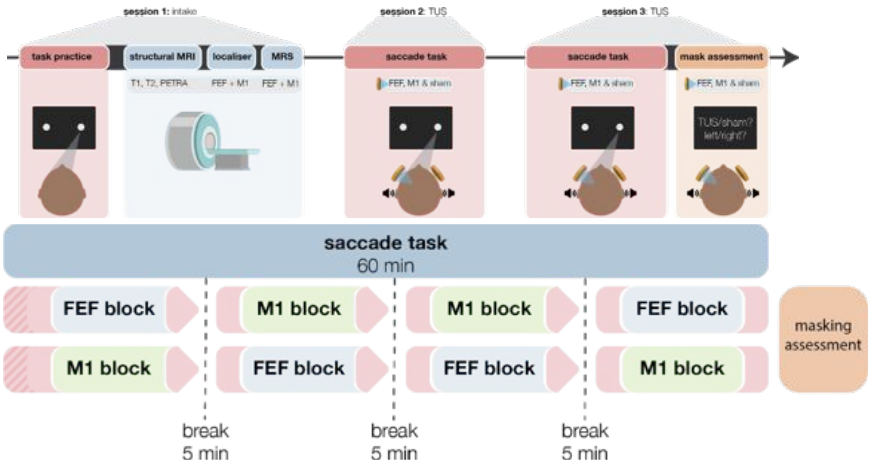

Figure 2 | Overview study design. (A) Structure of the three-part study, consisting of an intake session and two brain stimulation session. (B) Two TUS-block sequences with specific orders of the FEF-blocks and M1-blocks. Sequences of TUS blocks determined the placement of the two TUS transducer. After the 5-minutebreak, neuronavigation was performed to reposition the two TUS transducers and eye trackerwas validated and calibrated.

Tasks

Saccade task

Participants were instructed to fixate on a star-shaped stimulus (visual angle,0.25 x 0.25 degrees) presented at the centre of the screen. After fixation, two planet-shaped targets (visual angle, 0.5 x 0.5 degrees, acceptance window, 3 degrees) appeared sequentially in each hemifield (visualangle, 10 degrees left and right from the centre of the screen), with target onset delays ranging from 0 to 200 milliseconds. The distribution of target onset delays followed a normal distribution, with shorter target onset delaysclustered around the central peak and the longer targetonset delays at the tails.This distribution aimed to capture potential TUS-induced behavioural modulation, particularly at shorter target onset delays.Participants were then instructed to execute a saccadic eye movement to the first appearing target in either the left or right hemifield. Feedback followed each trial, indicating whether the correct target had been chosen within the designated time (Figure 3A). The task was gamified, allowing participants to earn points and a monetary bonus of up to €5 per stimulation session depending on their overallperformance. The saccade task lasted 60 minutes, with five-minute breaks after each TUS block.

During both the saccade task and TUS delivery, participants wore bone-conducting headphones (AfterShokz, New York, US) through which the auditory mask was played. This sound was designed to blind participants to various stimulation conditions and minimise putative auditory confounds. The design included white noise and layered smooth waves, tailored to either mask or replicate the sound for TUS and sham trials, respectively (Figure 3B).

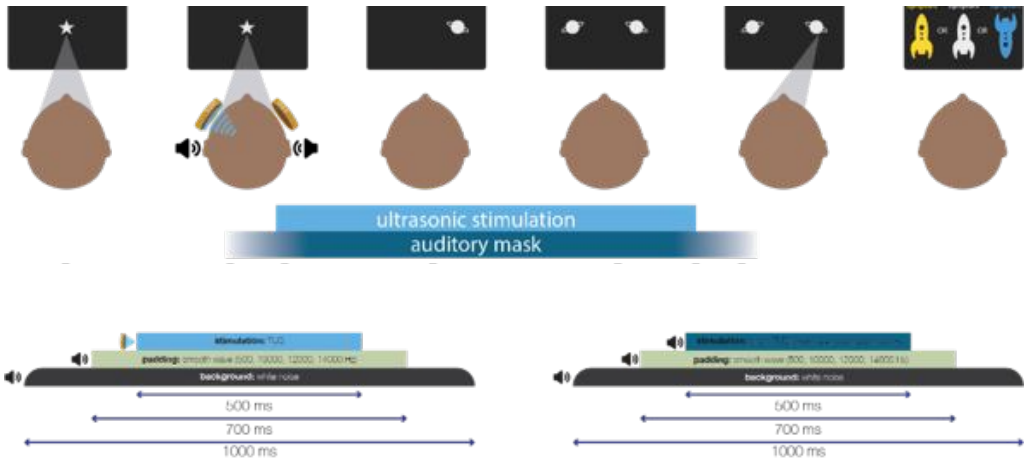

Figure 3 | Timeline saccade task. (A) Participants fixated on a central stimulus. A target appeared in the left or the right visual hemifield. After a brief variable target onset delay (between 0 and 200 ms), a second target appeared in the other hemifield. Participants were instructed to make a

saccadic eye movement towards the target that appeared first and received feedback based on their performance followed each trial. TUS was delivered 200 ms before the appearance of the first target, with a total stimulation duration of 500 ms. The auditory mask covered the duration of stimulation with a total duration of 1000 ms. (B) The played auditory mask corresponded to the stimulation condition. It masked TUS trials by covering the stimulation sound with white noise and built-up smooth waves. To replicate the stimulation sound in sham trials, a third layer of built-up smooth waves was added.

Functional localisers

Functional localisers were utilised to obtain stimulation coordinates for each participant. The FEF localiser (Amiez et al., 2006; Gagnon et al., 2002) consisted of alternating 24-second blocks of saccadic eye movements and central fixation (Figure 4A). Participants followed and fixated on a target (visual angle, 1 x 1 degrees; white square; dark grey background; duration, 800 ms) presented at randomised screen positions— left, right, or centre (target distance, 14 degrees). This sequence of eye movement and fixation was repeated six times, allowing us to assess the contrast between active eye movement blocks and baseline fixation blocks, thereby identifying the FEFs. For the M1 localiser (Tzourio-Mazoyer et al., 2015), alternating 16-second blocks of left and right finger movement were implemented (Figure 4B). Participants were instructed to repeatedly pinch their index finger and thumb together within the 16-second interval, alternating between left and right hands for six blocks per hand. This task enabled the establishment of the contrast between finger movement for each hand, identifying the M1s.

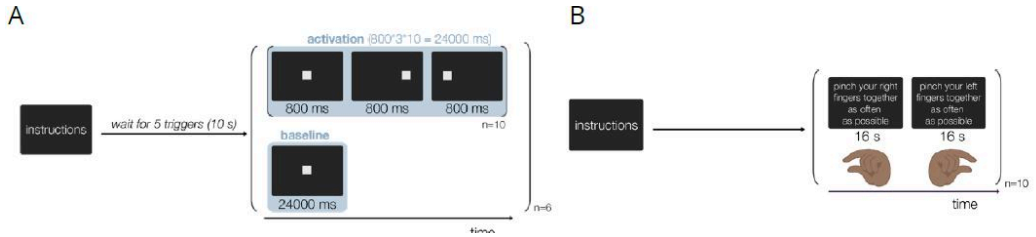

Figure 4 | Functional localiser tasks. (A) FEF localiser task required participants to follow a target presented randomly at the left, right, or centre of the screen for 800 ms, repeated 10 times. They also fixated on a central target for 24 s. Both tasks started after a delay of 5 volumes to accommodate signal steady-state transition and the haemodynamic response function following initial instructions at the screen. (B) During the M1 localiser task, participants repeatedly pinched their index finger and thumb together within 16 s.

Masking assessment

After the second stimulation session, participants experienced a shorter series of TUS (left and right FEF and M1) and sham trials. Following each trial, they were prompted to report whether they believed they had received stimulation and on which side they believed the stimulation had occurred. Unlike the pseudorandom order used in the saccade task, the order of the three stimulation conditions was fully randomised in this shorter series, given the reduced number of trials and the absence of behavioural modulation. Moreover, the TUS-block sequence with FEF-blocks and M1-blocks was counterbalanced across participants.

MRI data acquisition

MRI scanning was conducted at the Donders Centre for Cognitive Neuroimaging using a 3 Tesla Magnetom Skyra Scanner (Siemens AG, Erlangen, Germany) equipped with a 32-channel head coil. Participants were instructed to keep their eyes closed during the acquisition of structural scans. T1-weighted scans were acquired(sagittal plane; repetition time (TR), 2700 ms; echo time (TE), 3.69 ms; flip angle, 9 degrees; voxel size, 0.9 x 0.9 x 0.9 mm; field of view, 230 mm) for MRS voxel placement, co-registration with the functional data, and neuronavigation for TUS delivery. To capture detailed skull morphology and tissue properties, T2-weighted scans (sagittal plane; TR, 3200 ms; TE, 408 ms; flip angle, T2 var flip angle mode; voxel size, 0.9 x 0.9 x 0.9 mm; field of view, 230 mm), and Ultrashort Echo Time (UTE)scans (transversal plane;TR, 3.32 ms; TE, 0.07 ms; flip angle, 2 degrees; voxel size, 0.8 x 0.8 x 0.8 mm; field of view, 294 mm) were acquired. The T2-weighted and UTE scans will be utilised for future acoustic and thermal simulations.

To functionally localise the stimulation regions, a Multi-Band sequence with an acceleration factor of four (MB4; transversal plane; TR, 995 ms; TE, 32.8 ms; flip angle, 60 degrees; voxel size, 2.5 x 2.5 x 2.5 mm; field of view, 210 mm) was employed. Visual stimuli of the localiser tasks were presented at the rear bore face on a flat panel screen.

Lastly, Single Voxel Spectroscopy (SVS) using the MRS technique was performed in the left FEF and left M1. TUS has been shown to alter overall excitability by diminishing GABAergic inhibition while leaving Glu levels unaffected (animals: Yang et al., 2012; humans:Yakuub et al., 2023). To explore individual susceptibility to TUS, we assessedthe baseline GABA levelsin the stimulation regions, while baseline Glu levels will be examinedin the future. The SVS sequence started with shimming and MRS flip angle calibration, followed by voxel placement based on the participant's T1-weighted scan. Baseline level of GABA was measured using the pulse sequence MEshcher-GArwood Point RESolved Spectroscopy (MEGA-PRESS: TR, 2000 ms; TE, 68 ms; voxel size, 2.0 x 2.0 x 2.0 cm; with VAPOR water suppression 128 averages and water unsuppressed reference 16 averages), whereas baseline level of Glu was quantified using the pulse sequence Point RESolved Spectroscopy (PRESS: TR, 20000 ms; TE, 35 ms; voxelsize, 2.0 x 2.0 x 2.0 cm; with VAPORwatersuppression 64 averages).

Stimulation procedures

Preparation and neuronavigation

To prepare for neuronavigation and TUS delivery, we employed the MR-based Localite system (Localite GmbH, Bonn, Germany) to navigate through participant's brain morphology and target the obtained stimulation coordinates accurately. This system facilitated TUS delivery planning and provided real-time monitoring of transducer positioning throughout the entire stimulation sessions.

For neuronavigation preparation, we entered the participant's T1-weighted scan and x-, y-, z-coordinates of the left and right FEF and M1 obtained from the functionallocalisers into the Localite software. Head registration in the current space was achieved using a reference trackerand registering five markers at specific points on the participant's head (nasian, left and right eye, left and right ear), along with 350 – 400 markers of the head surface and circumference. Additionally, we calibrated the two TUS transducers using a referencetracker and calibration plate. This setup enabled the Polaris Spectra P7 camera to track head location relative

to transducers via infrared light. Positions of the transducers of the four stimulation regions were quantified for future acoustic and thermal simulations. For TUS delivery preparation, we applied ultrasound gel (Aquasonic 100, Parker Laboratories, NJ, USA) to the participant's scalp to ensurecoupling of the two transducers. Subsequently, we placed 1.5 mm thick gel pads (Aquaflex, Parker Laboratories, NJ, USA) between the gelled scalp and gel-covered transducers to eliminate air bubbles at the stimulation regions (Figure 5A).
During the stimulation sessions, we performed ongoing neuronavigation to monitor the positions of the two transducers throughout a TUS block.After each five- minute break, we repeated the neurnavigation process to reposition the two TUS transducers corresponding to the TUS-block type.

TUS protocol

TUS was delivered with the NeuroFUSPRO system (SonicConcepts Inc., Bothell,WA, USA; supplier/support: Brainbox Ltd., Cardiff, UK) equipped with two two-element ultrasound transducers (CTX-250, 45 mm diameter, Sonic Concepts Inc., Bothell, WA, USA) operating at a fundamental frequencyof 250 kHz. The utilisedTUS protocol was adopted from Kubanek et al. (2020) and was adjusted to modulate human behaviour (ramped pulse; pulselength, 1 ms; pulse repetition frequency, 500 Hz; total duration,500 ms; duty cycle, 50 percent; Isppa in free water, 25 W/cm2; Figure 5B). Our study used ramped pulses, which are squared pulses smoothed into a sinusoidal shape, in combination with an auditory mask to minimise auditory confounding. By contrast, Kubanek et al. used squared pulses and no auditory mask was played. Although squared and sinusoidal ramped pulses have the same integral energy content, it is important to note that squared wave pulses have associated limitations. A squared pulse encompasses a constant intensity peak for a longer duration due to their clear onset and offset, whereas a sinus-shaped pulse exhibits a gradually increasing and decreasing peak that is never fully off. Although low-intensity ultrasonic waves are beyond the range of human hearing,the on-offset of the squared pulse is detectable by humans, increasing the likelihood of auditory confounds, and thus contributing to a clearer temporal profile of stimulation. Furthermore, since humans have a thickerskull than macaques(Wu et al., 2014), a higher Isppa in water was applied. Moreover, we adjusted the total stimulation duration to the average human saccadeduration (Baizer & Bender, 1989). The temperature rise (ΔT) remained below two degrees Celsius and the derated intracranial mechanical index (MI) below 1.9 accordingto international regulatory regulations and the US Food and Drug Administration (FDA;Ng, 2002).

Behavioural acquisition

To record saccadic eye movements of the participant's dominant eye, we utilised the EyeLink 1000 PLUS eye tracker (SR Research Ltd.), positioned 70 cm away from the participant using a chinrestsetup (Figure 5C). Before commencing the saccade task, we conducted a nine-target calibration and validation procedure. The saccade task stimuliwere programmed using PsychoPy 2021.2.3 and presented on a 24-inch BenQ monitor (resolution, 1920 x 1080;refresh rate, 120 Hz; QisdaCorporation, Taipei, Taiwan).

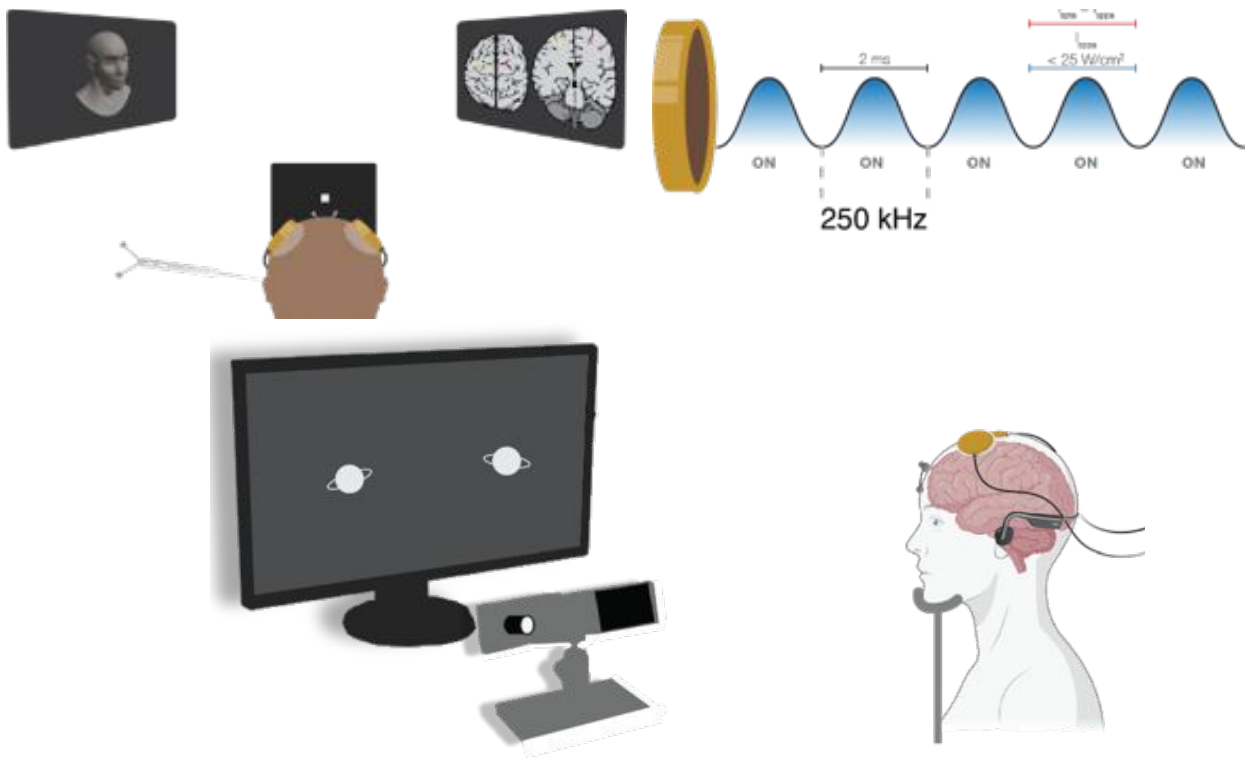

Figure 5 | Procedures brain stimulation sessions. (A) Neuronavigation involved registering the participant's head location and shape in the current space in relation to the calibrated TUS transducers. Coupling of the two TUS transducers required applying ultrasound gel on the participant's scalp, a gel pad for each transducer, and ultrasound gel on the transducer for optimal conductivity. Continuous neuronavigation monitored the positions of the two transducers throughout TUS blocks. (B) TUS protocol featuring ramped pulses. Squared pulses were smoothed into a sinusoidal shape to preserve the sum of energy. (C) Experimental setup with the participant performing the saccade task while recordingsaccadic eye movements, and coupling of the two TUS transducers to the participant's scalp at the stimulation regionmatching the TUS-block sequence.

Data analysis

Behaviour

For all our behavioural analyses, we utilised R (version 4.1.2; R Core Team, 2021) and RStudio (version 2021.9.2.382, RStudio Team, 2021). Given the repeated measures within participants, along with the hierarchical design involving multiple levels of experimental manipulation within participants (starting from the second behavioural analysis), we employed mixed-effects logistic regression models using glmer function with the logit link of the binomial family within the lme4 package (version 1.1.28; Bates, Maechler, Bolker, & Walker, 2015). To determine the random effect structure, we followed Barr et al. (2013) recommendation for maximal random-effect structure. All behavioural models featured a random intercept and a random slope for the respective independent variable(s) varying within participants.We compared various optimisers to achieve the best model fit using the log likelihood, with the 'bobya' optimiser providing the optimal fit across all behavioural models. We rigorously tested the models for singularity and convergence warnings and assessed assumptions for linearity, homoscedasticity, normality of residuals, and influential values using Cook's Distance..

No assumptions were violated, and adjustments were made accordingly if necessary. Subsequently, we computed confidence intervals (CIs) for the partial effects,regression coefficients, and interactions at an alpha-level of .05, .01, and .001 using the bootMer function of the lme4 with model-based parametric bootstrapping. For the last three behavioural models including TUS delivery during the saccade task, Wald-based CIs were computed using the car package (version 3.0-11; Fox et al., 2021), due to computational complexity. Furthermore, p-values assessing the overall contribution of eachpredictor to the model's fit were obtainedusing Type 3 conditional F-testswith Kenward-Roger approximation for degrees of freedom, implemented in the Anova function of the package car, which calls the KRmodcomp of the package pbkrtest (version 0.5.1; Halekoh & Højsgaard, 2014). For accessing all behavioural analyses,simply pastethis HTML file into your web browser's URL bar:file:///Users/Solenn/surfdrive2/saccade_task/analysis_scripts/solenn/Notebook_AllDataAnalyses.html

Baseline performance saccade task

To evaluate the efficacy of the saccade task, our primary goal was to establish a robust relationship betweenthe target onset delays betweenthe two targets and probability of the participants executing a saccadic eye movement towards a specific visual hemifield, referred to as saccadic direction (Figure 6). In short, the effects oflateralised TUS of the FEFs on the degree of rightward versus leftward saccades. This initial analysis involved behavioural data prior to TUS delivery (N = 23). Our hypothesis posited that longer target onset delays would result in a higher probability of a specific saccadic direction, attributed to early and robust evidence accumulation. Conversely,shorter target onset delays were expected to lead nearly equal probabilities across saccadic directions due to slower evidence accumulation. The mixed-effects logistic regression modelwas as follows:

$$probability\ rightward\ fixation \sim 1 + target\ delay + (1 + target\ delay \mid participant)$$

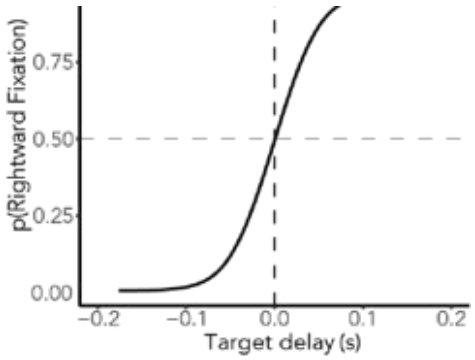

Figure6 | Relationship between target delay and probability of a specific saccadicdirection. The x-axis represents the target onset delays, rangingcontinuously from 0 to 0.2 s. Negative values indicate that the left target appeared first, while positive values indicate that the right target appeared first, with large values representing longer target delays. The y-axis, the probability of a rightward saccades is represented. As saccadic directionis dichotomous, a value of 0.50 suggestsan equal probability of executing a saccade in any direction. Values above .50 indicatea higher probability of rightward saccades,whereas values below .50 suggest a higher probability of leftwardfixations. The sigmoidal shape illustrates the relationship, with the bias for a specific saccadic direction represented by the curve's horizontal shift and certainty for a specific saccadic directionindicated by the curve's steepness.

Neuromodulatory TUS effects

After establishing the relationship between the target onset delays and probability of executing rightward saccades, particularly during the shorter target onset delays, we conducted a subsequent analysis using a subset of the behavioural data that included TUS delivery(N = 8). This subset was similarly pre-processed as the primarybehavioural analysis. Additionally, we omitted practiceand baseline trials,and factorised all stimulation conditions. Our hypotheses posited lateralised TUS of the FEFs may bias saccadicdirection. Given the lateralised relationship between neural activityand behaviour, this bias might enhance evidenceaccumulation, increasing the ratio for contralateral saccades, indicative of an excitatory effect (Figure 7A). Alternatively, TUS might diminish evidence accumulation for one target, increasing the ratio for ipsilateral saccades, suggesting an inhibitory effect (Figure 7B). Another outcome might be a perturbatory effect, attributed to distorted balance of evidence expressed in decreased saccadicaccuracy (Figure 7C).

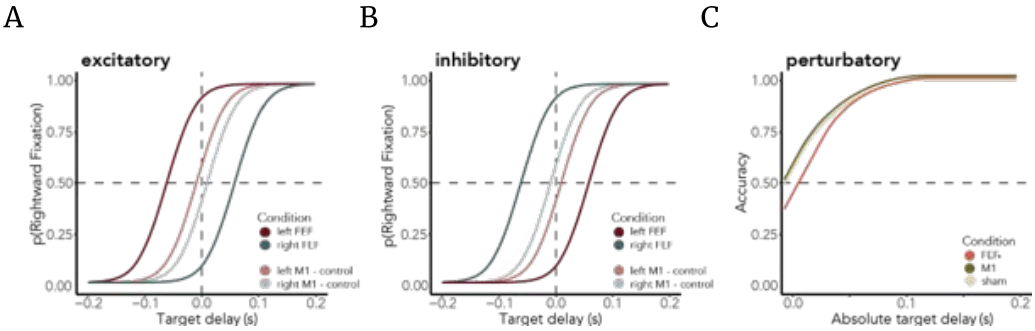

Figure 7 | Hypotheses for the neuromodulatory effect of TUS of the FEFs. (A) Excitatory bias effect is characterised by a horizontal shift of the curve from the expected baseline performance towards the contralateral hemifield relative to the side of stimulation, particularly noticeable at a target onset delay of 0 s. (B) Inhibitory bias effect is characterised by a horizontal shift of the curve from the expected baseline performance towards the ipsilateral hemifield relative to the side of stimulation, particularly noticeable at a target onset delay of 0 s. (C) Perturbatory bias effect is characterised by decreased saccadic accuracy. To focus on the critical comparison of TUS between the left and right FEF, we initially modelled the stimulation sides.The stimulation sideswere coded using a sum-to-zero contrast, with the left side as +1 and the right side as -1. This analysis was continued with the setupof the primary behavioural model:

probability rightward fixation ~ 1 + *target delay* + *side TUS FEFs* + (1 + *target delay* + *side TUS FEFs* | *participant*)

In addition to the mutual control within the FEFs, we included TUS of the left and right M1, hypothesising no bias for specific saccadic direction as they served as active control (Figure 7A-B). Stimulation regions were codedusing sum-to-zero contrast(FEF coded as +1 and M1 as -1). We also explored potentialinteractions between the target onset delays, stimulation regions, and stimulation sides, to gain insights into their combined influence on saccadic directions:

probability rightward fixation ~ 1 + *target delays* ∗ *stimulation regions* ∗ *stimulation sides* + (1 + *target delays* ∗ *stimulation regions* ∗ *stimulation sides* | *participant*)

We further explored potential biases, whether excitatory or inhibitory, at the single- subject level (refer to Supplemental materials). This analysis comprised two main components: first, a Bayesian logistic regression model employing the Bernoulli family in conjunction with the identity link; second, iteration of the Bayesian model 10,000 times, with computation of marginal means for the bias parameter per stimulation condition. These analyses were conducted using the brms package (version 2.16.3; Bürkner, 2017) and emmeans package (version 1.1, Lenth et al., 2018). This preliminary setup of single- subject analysis laid the groundwork for the development of a hierarchical Bayesian logistic regression model, intended for future use, which will merge the initial two-fold analysis.
Our data analysis extended Kubanek et al.'s data analysis, allowing us to explore potential perturbatory neuromodulatory effect. Specifically, we assessed the saccadic accuracy as a function of the interaction between absolute target onset delays and stimulation conditions. Given that the dependent variableis not lateralised, we aggregated target onsetdelays and stimulation conditions across sides.This included the hemifields in which the targets appeared, with absolute targetonset delays as result, and the hemispheres in which TUS was delivered, respectively. Stimulation conditions were coded using sum-to-zero, with pooled FEF coded as 0, pooled M1 as +1 and sham as -1):

accuracy ~ 1 + *absolute target delay* ∗ *stimulation conditions* + (1+ *absoluate target delay* ∗ *stimulation conditions* | *participant*)

To explore if the potential reduced accuracy differed between stimulation sides, we added stimulation sides to the interaction of the former model. Sham trials were omitteddue to the hierarchical structure. Left was coded as +1 and right as -1:

accuracy ~ 1 + *absolute target delay* ∗ *stimulation conditions* * stimulation sides + (1 + *absoluate target delay* ∗ *stimulation conditions* * stimulation sides | *participant*)

Functional localisers

We processed fMRI data using SPM12 in Matlab R2023a, along with FSLeyes forresult visualisation. Initially, we excluded the first five fMRI volumes to allow for signal steady-state transition, converted IMA files to DICOM compatible format, and visually checked for artefacts. Both single-subject and group-level analyses(N = 17) were performed to establish stimulation coordinates within native space (i.e., not normalisedto standard MNI space) and standard space,respectively.
Realignment and re-slicing of the functional data were performed for both levels, followed by co-registration with the participant's T1-weighted image for single-subject analysis and with Montreal Neurological Institute(MNI) standard space for group-level analysis. Smoothing with a six mm full-width at half-maximum (FWHM) Gaussian kernel was applied to both levels, and realignment parameters per participant were inspected. The block design was convolved with canonical hemodynamic response function, followedby voxel-wise fittingof a general linear

model (GLM), resultingin the computation of statistical parametric maps for comparisons. Subsequently, beta weights for each condition were estimated to create contrast maps, enabling Family-Wise Error corrected cluster-level inferences ($p < .05$).For the FEF localiser, the contrast of following a target minus fixation was utilisedto obtain stimulation coordinates for the left and right FEF. We selected a peak voxel within the significant cluster, specifically at the junction of the superior precentral sulcus and the superior frontal sulcus (Amiez et al., 2006; Gagnon et al., 2002).

Importantly, the FEF localiser task required reflexive pro-saccades, activating both medialand lateral FEF peaks. The medial peaks, associated to higher-order cognitive control of voluntary saccades (Cameron, Riddle, &D'Esposito, 2015; Curtis,2006; Curtis &D'Esposito, 2006; Gagnon et al., 2002; Neggers et al., 2012; McDowell et al., 2008) were selected for stimulation targets.The M1 localiser contrast involvedpinching right fingersminus left fingers and vice versa to identify the left and right M1, respectively, eliciting a distinctive activation cluster of significant voxels in both left and right M1. For both FEFs and M1s, the local maximum of peak voxel within the activation cluster was selected for the x-, y-, and z-stimulation coordinates.
The accuracy of selected coordinates within sulci branches was assessed with FSLeyes by visualising effect sizes modulated by statistical significance with transparent threshold. Once confirmed, established coordinates per stimulation region were entered in the Localitesoftware to plan and monitorTUS delivery. Group-level analysis calculated the contrast estimates' standard error and mean, determining significanceof the average estimate and was visualised with MNI152 T1-weighted template.

Auditory mask effectiveness

The effectiveness of the auditorymask in blinding participants to various stimulation conditions and minimising putative auditory confounds was assessed. Wehypothesised that the auditory mask effectively masked or replicated the auditory stimulation, irrespective of the presence of stimulation and stimulation sides. The mixed- effects logistic regression models focused on the participant's ability to differentiate between sham (coded as +1) and TUS stimulation (coded as -1) both aggregated across the stimulation regions and stimulation sides, and if they did so accurately:

response stimulation ~ 1+ *given stimulation* + *accuracy response side* + (1 + *given stimulation* + *accuracy response side* | *participant*)

We also evaluated participant's ability to differentiate between left (coded as +1) and right stimulation (coded as -1) both aggregatedover stimulation regions, and determineif they did so accurately:

response left *side* ~1 + *given side* + *acuracy response side* + (1+ *given side* + *accuracyresponse side* | p*articipant*)

Baseline GABA level

We assessedthe potential relationship baseline GABA concentrations in institutionalised units(IU) within the left stimulation regions on the perturbatory effects on saccadic accuracy toexplore potential individual susceptibility to TUS (refer to Supplemental materials).

Results

Behaviour

Baseline performance saccade task

We employed a mixed-effects logisticregression model to establish the relationship between target onset delays on specific saccadic direction probabilities.Our hypothesis, whichproposed longer target onset delays would favour a specific directionwhile shorter target onset delays would lead to uncertainty, was supported.

Participants showed a higher probability of rightward saccadeswhen the first target appearedin the right hemifield (Estimate = 0.03, SE = 0.00,99.9% CI [0.02, 0.04], F(21) = 302.58,p < .001, Figure 8), demonstrating the task's effectiveness.

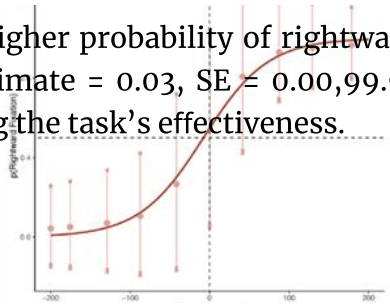

Figure8 |Baseline performance saccade task. Mean probabilities (± SD) per target onset delay bin, along with the fitted sigmoid curve, illustrate that the probability of a specific saccadic directionincreased with longer target onset delays whereasshort target onset delays resultedin larger SDs and an equal probability of any saccadicdirection at a target delay of 0 s.

Neuromodulatory TUS effects

When exclusively considering TUS delivery to the FEFs during the saccade task, our mixed-effects logistic regression model replicated the robust findings of our primary behavioural analysis.Specifically,we observed that the probability of executing a rightward saccades increased with longer target onset delays (Estimate = 0.04, SE = 0.00, 99.9% CI [0.02, 0.05], F(7) = 37.65, p < .001, Figure 9A). Moreover, our analysis revealed a finding regarding the crucial effect of TUS on saccadic directions. Specifically, we found that the probability of rightward saccades increased with TUS of the left FEF, when considering independently (Estimate = 0.13, SE = 0.06, 95% CI [0.01, 0.25], p = .02, Figure 9B-C), suggesting an excitatory effect. However, when accounting for its combined effects with TUS of the right FEF and target onset delays, the significance of FEF stimulation side diminished (F(7) = 3.03, p = .125). Moreover, TUS of the right FEF elicited a sigmoid curvesimilar to baselineperformance without TUS delivery.

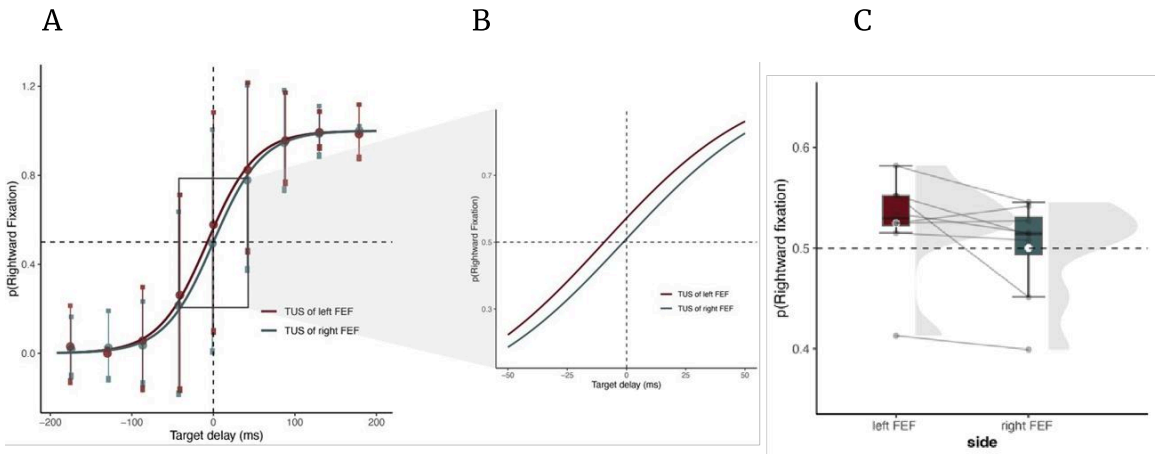

Figure 9 | Effects of TUS of the left and right FEF on saccadic direction.(A) Mean probabilities (± SD) per target onset delay bin, along with the fitted sigmoid curve, show that the probability of a specific saccadic direction increased with longer target delays. (B) The zoomed-in fitted sigmoid curve focused on shorter target onset delays (-50 to 50 ms), highlighting the potential influence of TUS on saccadic direction. The leftward horizontal shift of TUS of the left FEF relative to baseline performance at a target delay of 0 s suggests an excitatory TUS effect on contralateral saccades. (C) Boxplots and violin plots illustrate the probability of rightward saccades as a function of FEF stimulation sides aggregated across all target onset delays.

We extended our analysis to include lateralised TUS of the M1s as active control and examined the interaction between target onset delays, stimulation regions, and stimulation sides on saccadic direction using a mixed-effects logistic regression model. We replicated the effect of target onset delays (Estimate = 0.04, SE = 0.00, 99.9% CI [0.03, 0.04], F(7) = 531.14, p < .001, Figure 10A). Furthermore, when considered independently, TUS of the left FEF maintained its significant association with an increased probability ofrightward saccades (Estimate = 0.14, SE = 0.04, 99.9% CI [0.03, 0.24], p = .001, Figure 10B- C), suggesting an excitatory effect. However, the Type 3 conditional F-test revealed no effect of stimulation side on saccadicdirection probability when considering the combined effect with TUS of the right FEF, target onset delays and stimulation regions (F(7) = 3.03, p = .159). Similarly, stimulation regions, both independently and when adjusting for other predictors, did not show significance (Estimate = 0.02, SE = 0.00, 95% CI [-0.07, 0.12], p = .55, F(7) = 0.00, p = .86, Figure 10B-C). Moreover, none of the interactions between target onset delays, stimulation sides, and stimulation regions were significant, either individually or collectively when considered within the complete model. This suggests that the effect of TUS of FEF on saccadic direction, relative to TUS of M1, with target onset delays did not differ between left and right, indicative of a consistent relationship across target onset delays, stimulation sides, and stimulation regions. Refer to Supplemental materials (Table S2, Figure S1) for results at single-subject level.

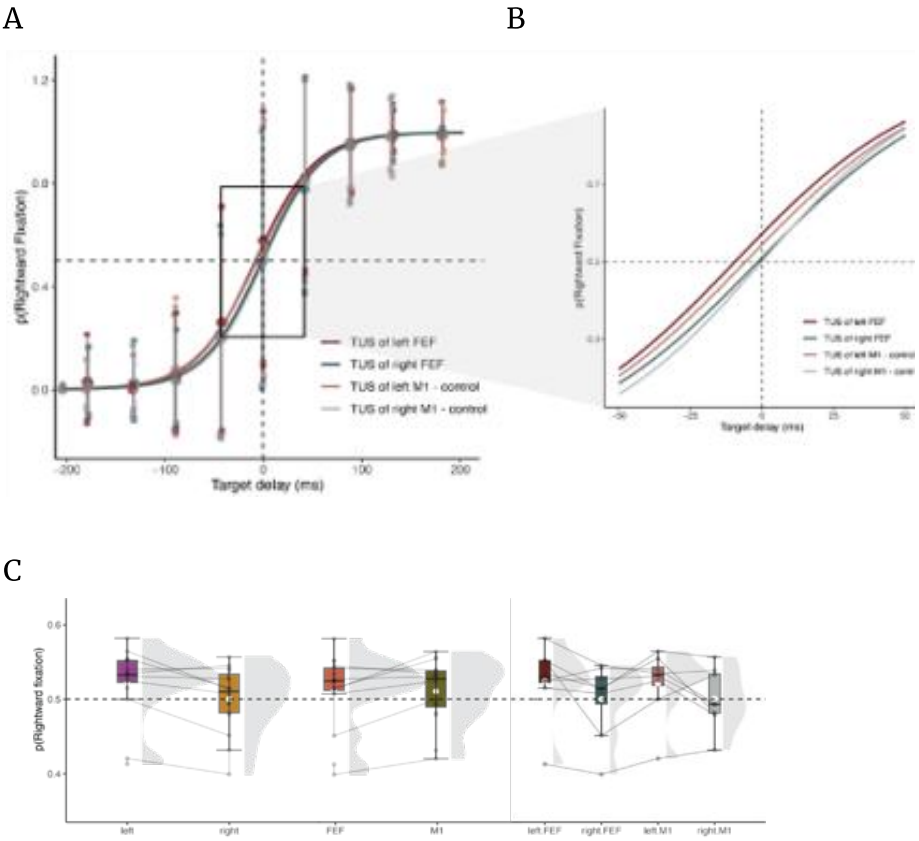

Figure 10 | Effects of TUS of the left and right FEFs and M1s on saccadic direction. (A) Mean probabilities (± SD) per target onset delay bin, along with the fitted sigmoid curve demonstrate that the probability of a specific saccadic direction increased with longer target onset delays. (B) The zoomed-in fitted sigmoid curve focused on shorter target onset delays (-50 to 50 ms). The leftwardhorizontal shift observedin all left-sided stimulations relativeto baseline performance at a target onset delay of 0 s suggests an excitatory effect of TUS on contralateral saccades, irrespective of specific stimulation regions. However, when considering the combined effect with the other predictors, no discernible horizontal shift is evident between stimulation sides and stimulation regions. (C) Boxplots and violin plots depict the probability of rightward saccadesbased on each stimulation side aggregated across all stimulation regions, each stimulation region aggregated across all stimulation sides and interactions between stimulation sides and stimulation regions, aggregated acrossall target onsetdelays.

Another possibility is that TUS of the FEFs did not enhance or diminish evidence accumulation processing but instead disruptedthe balance of evidence, leadingto decreased saccadic accuracy. The mixed-effects logistic regression model revealed that saccadic accuracyincreased with longertarget onset delays(Estimate = 0.04, SE = 0.00, 99.9% CI [0.03, 0.05], F(7) = 1551.93, p < .001, Figure 11A). Moreover, when examined independently, saccadic accuracy decreased with TUS of the FEFs relative to sham (Estimate = -0.15, SE = 0.06, 99.9% CI [-0.27, -0.03],p = .02). However,when considering stimulation condition in its entirety together with absolute target onset delays, this effect diminished in significance (F(6) = 3.85, p = .08, Figure 11B-C).

Additionally, the interaction between targetonset delays and stimulation conditions did not have an effect on saccadic accuracy (F(6) = 2.55, p = .16, Figure 11B-C), suggesting that the relationship between target onset delays and saccadic accuracydid not vary across stimulation conditions.

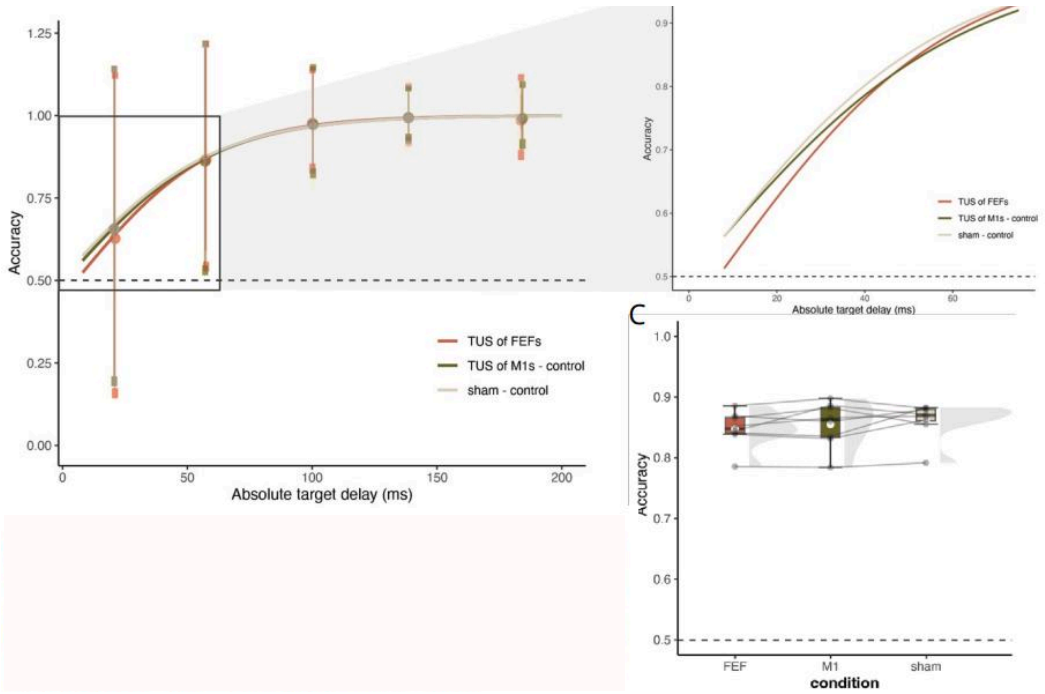

Raw means (± SD) and fitted sigmoid curves of the stimulation conditions show TUS of FEFs leads to saccadic accuracy below chance level, potentially indicative for decreased saccadic accuracy induced by TUS of FEFs (B) Zoomed in sigmoid curve on short target delays (0 ms to 75 ms), suggesting decreased accuracy for TUS of left FEF. (C) Box- and violin plots of raw data show stimulation conditions averaged across all target delays per participant as a function of saccadic accuracy.

Given the observed decrease in saccadic accuracy with TUS of the FEFs compared to sham, we continued exploring if the decreased accuracy differed between stimulation side, controlled by lateralised TUS of the M1s. None of the main effects (p >.19) or partial effects (p > .13) for the stimulation sides, stimulation regions, or their interaction reached statistical significance. Despite these non-significant findings, we visually inspected the results to gain insights into potential trends, especially as the data acquisition of the full sample size was not reached yet. We dividedaccuracy based on the targetthat appeared first duringvery short targetonset delays corresponding to each hemifield.

When the left target appeared first, both left and right FEF stimulation appeared to decrease saccadic accuracy (Figure 12A-B). TUS of the left FEF decreased saccadic accuracy for the left target attributed to a flatter steepness across absolute target onset delays. Remarkably, TUS of the right FEF on the other hand initially exhibited the lowest accuracy for the left target, up to 20 milliseconds, but then rapidly improved accuracy relative to TUS of the left FEF as the absolute target onset delays increased. This latter suggests that TUS of the right FEF at very short target onset delays specifically might decrease accuracy.

Conversely, when the right target was presented first, TUS of the left FEF did not appear to diminish accuracy compared to TUS of the right FEF (Figure 12C-D). This finding supports the concept of contralateral excitability and is consistent with our previous results from TUS of the left FEF on both saccadic direction and accuracy. Moreover, TUS of the right FEF once more appeared to reduce accuracy at short target onset delays compared to lateralised TUS of the M1s, this time in a consistent steepness manner across target onset delays.

A B C D

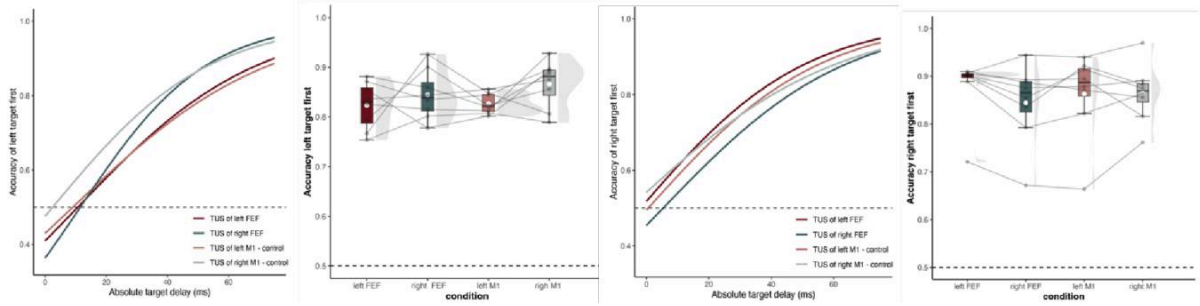

Figure 12 | Effects of TUS of the left and right FEFs and M1s on saccadic accuracy. (A-C) The zoomed-in unidirectional sigmoid curve illustrate the saccadic accuracy when the left (A) or right (B) target appeared first during very short absolute target onset delays (0 ms to 75 ms). (B-D) Boxplots and violin plots of depict saccadic accuracy when the left (B) or right (D) target appeared first as a function of the interaction of stimulation region and stimulation side, aggregated across target onset delays.

Functional localisers

We tailored the localisation process for each participant to account for inter- individual variability in brain morphology and ensure precise neuromodulation, therebyenhancing the efficacy of our onlineTUS protocol. At the group level, the strongest clusteractivations representing the FEFs were observed along the precentral sulci (Table 1, Figure 13A-B). However, upon closer examination in three planesand analysis of single- subject data (Figure 13E), we identified a complex comprising two distinct activations within the cluster, which may appear as a single continuous activation at the group level. Consistent with prior studies (Amiez et al., 2006; Gagnon et al., 2002; Gitelman et al., 2000; Petit et al., 1997; Shulmanet al., 1999), we observedindividual variations withinthe FEFs, pinpointing two distinct peak activations; a lateral and a medialone, of which we opted to target the medial peak to stimulate voluntary saccadic eye movements (Cameron, Riddle, & D'Esposito, 2015; Curtis, 2006; Curtis & D'Esposito, 2006; Gagnon et al., 2002;Neggers et al., 2012). This medial peak is located at the intersection of the superior precentral sulcus and the superior frontal sulcus, particularly at the junction of the dorsal and ventral branch of the superior precentral sulcus (Figure 13B-C), replicating Amiez et al. (2006).

In contrast, the M1 localiser revealed clear activation clusters at both group-(Table 1, Figure 13 F-G) and single-subject level (refer to Table S1 in Supplemental materials, Figure 13 H-I). The M1s are locatedat the intersection of the dorsal branchof the superior precentral sulcuswith the superiorfrontal sulcus, extending dorsally.

Table 1 Functional localisercoordinates at group level

Contrast.	ROI	*X* (mm)	*y* (mm)	*Z* (mm)	$t_{(288)}$ value	cluster size
follow – fixation	left FEF	-24 ± 7.11	-7 ± 9.50	50 ± 12.33	11.56	27
follow – fixation	right FEF	39 ± 4.47	-4 ± 10.66	47 ± 12.28	13.53	37
					$t_{(192)}$ value	
right fingers – left fingers	left M1	-36 ± 4.52	-22 ± 19.72	53 ± 11.69	11.42	122
left fingers – right fingers	right M1	36 ± 4.60	-19 ± 10.11	53 ± 13.46	12.26	76

Abbreviations: ROI = region of interest; FEF = Frontal Eye Field; M1= primary motor cortex, hand area
Note: MNI coordinates for functional localiser task. Significance level for all cluster listed is $p_{FWE} < .05$.

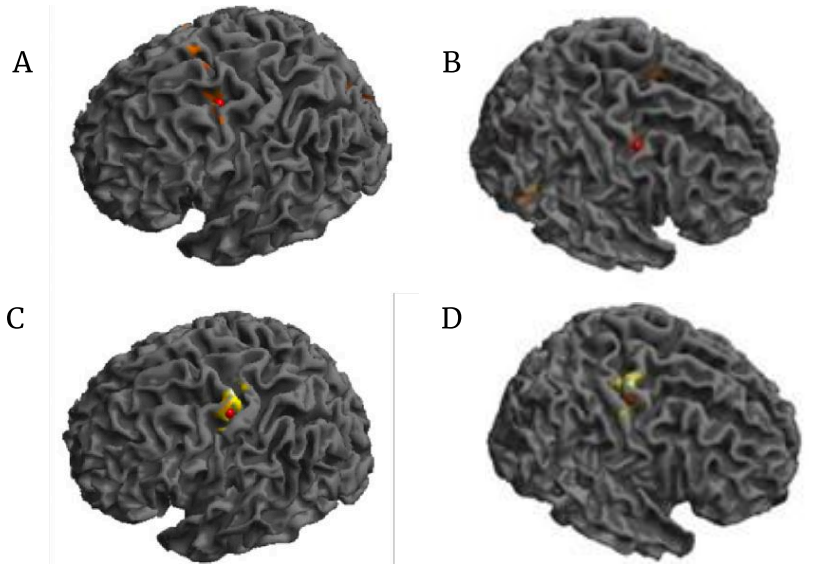

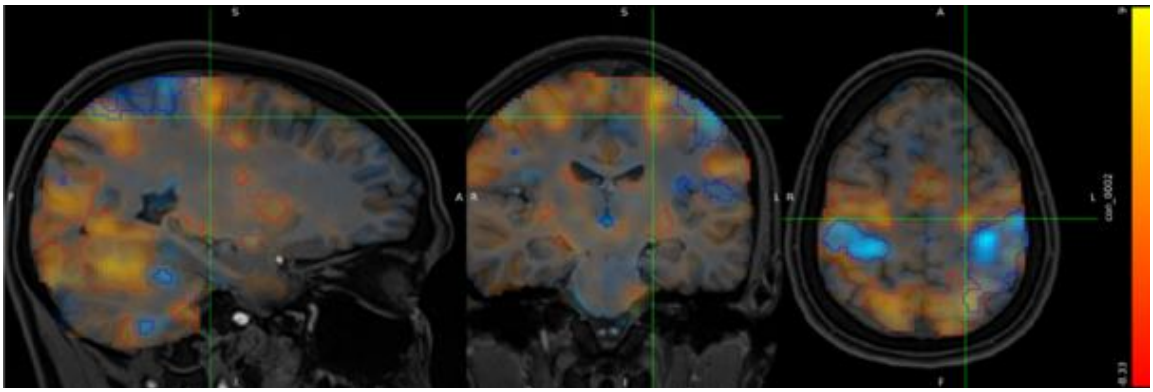

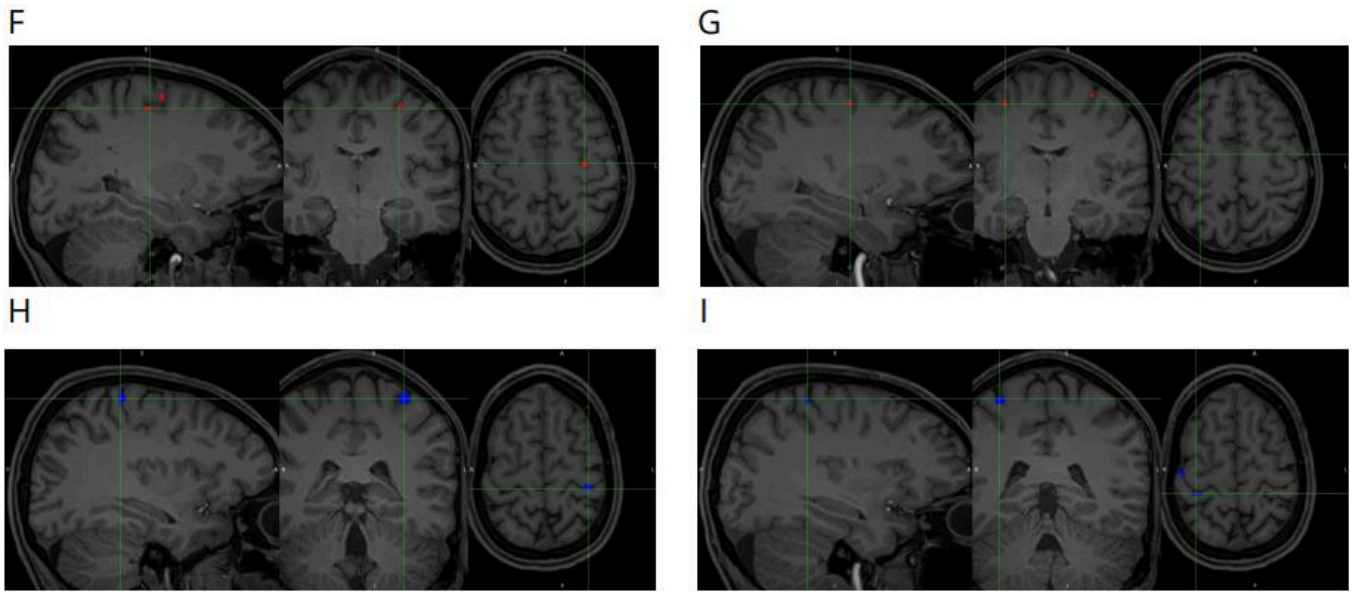

Figure 13 | Functional localisation of the left and right FEF and M1. Group-level. A-B) Averaged MNI coordinates for the left (A) and right FEF (B) are positionedat the junction of the dorsal and ventral branch of the superior precentralsulcus and the superior frontal sulcus, as displayed in the MNI render. (C-D) Averaged MNI coordinates for the left (C) and right (D) M1 are located at the intersection of the dorsal branch of the superiorprecentral sulcus with the superiorfrontal sulcus, extendingdorsally, as displayedin the MNI render. Single-subject. I. Anatomical, effect, and statistical images of the left and right FEF and M1 overlayed for visualisation of anatomy, with less significant effect values depictedtransparently to highlightthe most important effect voxels, alongsidean outline of the statisticswith a specified threshold. (F-I) Anatomical and statistical images of the left and right FEF (F-G) and left and right M1 (H-I). The threshold of the statistical image (red) was maximised to assess the accuracy of the established coordinates (green crosshair) in locating the expected branches of the sulci given the participant's morphology. Note radiological orientation.

Auditory mask effectiveness

A mixed-effects logistic regression model assessed the effectiveness of auditory masking, revealing that participants were inclined to believe they could discern between sham and TUS trials (Estimate = -2.46, SE = 0.39, 95% CI [-3.22, -1.69], F(6.90) = 90.58, p < .001). Specifically, they appeared to be confident they were not stimulated when receiving sham, but highly prone to guessing that they were stimulated when receiving TUS. However, they were unable to accurately distinguish between the stimulation conditions (Estimate = 1.92, SE = 2.05, 95% CI [-2.09, 5.94],F(6.99) = 1.08, p = .35, Figure 14A).

Similarly, participants' perception of the stimulation side they believed they were being stimulated on differed (Estimate = 2.45, SE = 1.09, 95% CI [0.26, 6.44], F(5.95) = 7.88, p = .03). However,the perception appearedto be a slight bias towards believingthey were stimulated on the right side even when the stimulation was delivered on the left side. Moreover, participants struggledto accurately identifystimulation sides (Estimate = 3.35, SE = 1.58,95% CI [-1.27, 4.35], F(5.64) = 4.08,p =.09, Figure 14B).

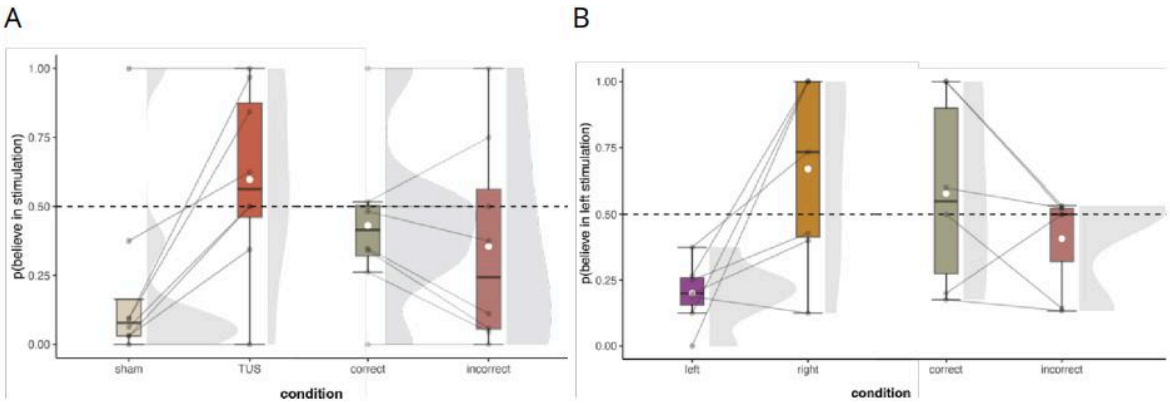

Figure 14 | Auditory mask effectiveness assessment. (A) Boxplots and violin plots display participants' beliefs regarding whether they were stimulated, aggregated across stimulation regions and stimulation sides, along with their accuracy. Sham stimulation shows a clear distribution when participants believedthey were unlikelyto have been stimulated, while TUS exhibitsa spread distribution across belief probabilities. Participants were often correct when unsure about being stimulated, but incorrect beliefs were more varied, with a slight tendency toward incorrectness when they believed they were not stimulated. (B) Boxplots and violin plots depict participants' beliefs regarding which side they were stimulate ond, aggregated across stimulation regions, and their accuracy. Clear distributions are observed when participants believed they were unlikely to have been stimulated on the left side, while belief probabilities skewed toward stimulation on the right side. Correct beliefs show a spread across belief probabilities, while incorrect beliefs exhibit a clear distribution when participants were unsure if they had been stimulated, with a slighttendency toward believingthey had not been stimulated.

Baseline GABA level

No correlation was found between GABA baseline levels and individual susceptibility to neuromodulation, based on five participants (refer to Supplemental materials, FigureS2).

Discussion

In this study, we aimed to establish an effective online TUS protocolfor human use, with the focus on gaining insights into the neuromodulatory effects of TUS and disentangling between excitatory, inhibitory, and perturbatory effects. Specifically, we investigated the effects of lateralised TUS of the FEFs on lateralised saccadic direction and accuracy in a lateralised choice task. To this end, eight participants completed all three parts of the study, with a design focused on maximising the protocol's efficacy while minimising confounding factors.

First and most importantly, TUS delivered to each FEF independently influenced saccadic direction and accuracy during shorter target onset delays.TUS of the left FEF led to a higherprobability of rightward saccades, implying an excitatory effect on saccadic direction. Moreover, accuracy decreased with lateralised TUS of the FEFs, particularly notable with right FEF stimulation, hinting at a potential perturbatory effect on saccadic accuracy.

However, the preliminary findings, based on limited data, are likely influenced by the small sample size. Nonetheless, the independent effects offer valuable insights into the unique contribution of specific stimulation sides on saccadicbehaviour. These insightsmay become more significant with a largersample size.

No evidence for TUS-induced bilateral bias on saccadicdirection

Unlike Kubanek et al. (2020) who demonstrated a 2:1 excitatory bias on saccadic direction resulting from TUS of both FEFs in non-human primates, we did not observe strong evidence for such bias with TUS of the left FEF or any bias induced by TUS of the rightFEF on saccadic direction.

Variations in methodology may interact with the putative mechanisms of TUS, potentially leading to divergent behavioural outcomes. For instance,our TUS protocol utilised sinusoidal ramped pulses and an auditory mask to minimise auditory confounds,whereas Kubanek employed squared pulses without an auditory mask. Their distinct on- offset of energy differs from our gradual modulation, which may impact neuronal depolarization by causing a more abruptinflux of calciumor sodium ions (Sorum et al., 2021; Yoo et al., 2022), or pressure changes in the cell membrane (Jerusalem et al., 2019; Yoo et al., 2022). Consequently, it is possiblethat squared pulses in Kubaneket al.'s studymight have had a more pronounced effect than our pulses. Additionally, we tailored ourpulse parameters for human participants, including a higher spatial-peak pulse-average intensity (Isppa) to penetrate the thickerhuman skull and a longerpulse duration to align with the longer duration of human saccades (Baizer & Bender, 1989). Conversely, while our pulse parameters were adjusted for human participants, they might have had a different effect comparedto those used by Kubaneket al.

As a result, these variations could potentially cause ultrasonic waves to either undershoot or overshoot, potentially affecting the anticipated observation of an excitatory bias from both the left and right FEFs.

Functional asymmetry within the FEFs

The absenceof evidence for any bias induced by TUS of the rightFEF on saccadic direction may stem from fundamental differences within the FEFs. One potential explanation could be asymmetrical resting-state functional connectivity within the FEFs. Hutchison et al. (2012)observed in humans that the right FEF seed—precisely localised as in our study (Amiez et al., 2006)—exhibited strong positive correlation with activity in the left FEF, while the left FEF seed did not show contralateral connectivity. This implies that TUS of the left FEF, with its more isolatedconnectivity, may inducelocalised TUS effects, enhancing evidence accumulation for rightward saccades. In contrast, TUS of the right FEF might propagate effectsto the left FEF, resultingin a less pronounced TUS effects. It is imperative to note that our TUS protocol consistently generates the same stimulation, differences observed in behavioural outcomes may arise from variation in functional connectivity within the stimulated region. Furthermore, considering the potential modulation of functional connectivity by TUS, Yaakubet al. (2023) demonstrated that offline TUS of 20 milliseconds theta burst pulses increased functional connectivity within targeted human frontallobe areas and networks afterapproximately 13 to 50 minutes.However, to date, no study has investigated how online TUS protocols with shorter pulse durations, in our case 1 millisecond, might modulate functional connectivity in humans, limitingour understanding of this possibility with our onlineTUS protocol.

Moreover, the disentanglement of excitatory effects on saccadic direction and perturbatory effects on saccadicaccuracy align with previous TMS studies targetingFEFs during attentional tasks (Grosbas & Paus, 2002, 2003; Hung et al., 2011). Similarly, TMS of the left FEF exhibited effects on contralateral targets,whereas TMS of the right FEF led to effects both on ipsilateral and

contralateral targets. These findings suggest that TMS of the right FEF disruptstop-down control in visual processing, consistent with right hemisphere dominance for visuospatial abilities and attention (Guarriglia et al., 1993; Husain et al., 2000; Heilman & Valenstein, 1972; Heilman& Van Den Abell, 1980).Despite the potential for producing similar behavioural effects due to the susceptibility within the FEFs to neuromodulation, it is important to highlight that TMS and TUS have distinct mechanisms and effects.

From another perspective, visualisation suggests that TUS of the right FEF could potentially have a perturbatory effect on saccadic accuracy, particularly evidentat very shorttarget onset delays.Unlike TUS of the left FEF, whichexhibited an influence on accuracy consistent with the putativecontralateral nature, TUS of the right FEF led to decreasedaccuracy regardless of the hemifield in which the first target appeared. Thissuggests that the effects of TUS of the right FEF on the contralaterality may cancel each other out, explaining its absence of any bias in saccadic direction and supporting the observed preliminary perturbatory effect on saccadicaccuracy induced by lateralised TUS of the FEFs. This divergent impact of TUS on the right FEF may also explain why only partial effectswere significant, in addition to the limiteddata.

Despite the mutual controlwithin the FEFs, it is vital to consider inherentcharacteristics unique to the stimulation region, in this case their functional connectivity, cognitive control, and visuospatial attention. These factors could result in unforeseen interactions with neural tissue and potentially less robust behavioral effects.

Evidence accumulation parameters

Our observations highlight the potential influence of TUS on saccadic behaviour, particularly evident during shorter target onset delays. While our hypotheses have shedlight on how this influence might involve enhancements and added randomness to the evidence accumulation process, the next pivotal step is integrating computational cognitive models,such as the drift diffusion model commonly employedfor 2AFC tasks.

For future work with drift diffusioin models, Kubanek et al. (2020) suggested that TUS may bias the starting balanced state even before a stimulus is presented (known asthe starting point), the speed of the drift towards a choice, or the choice threshold. These parameters could be associated to the excitatory effect. Conversely, the perturbatory effect may impact the behavioural parameters non-decision time or the level of noise in the choiceprocess. For instance, Grosbas and Paus (2003) demonstrated that TMS of the FEFs shortly before the target's onset, like our TUS protocol, enhanced visual sensitivity, including the effect of TMS of the right FEF on both ipsilateral and contralateral targetsas well. These findings suggest that neuromodulation of the FEFs might expedite sensory encoding, thereby reducing non-decision time. However, if this heightened sensitivity is not complemented by adjustments in other parameters, such as increased drift rate or threshold, it could introduce noise, potentially leadingto a perturbatory effect on saccadic accuracy.

By implementing and comparing thesecomputational cognitive models,we can delve deeper into which parameters and at which stages TUS influences choice making, providing a more nuanced understanding of the latent mechanisms and implications for cognitive function.

Caveats, considerations, and future directions

Our study design aimed to maximise the protocol's efficacy and minimising confounding factors, ensuring unequivocal inference from behavioural modulation and facilitating disentanglement between excitatory, inhibitory, and perturbatory neuromodulatory effects. We successfully validatedthe effectiveness of the saccadetask, confirmed the accuracy of the functional localisers for neuronavigation, and effectively controlled TUS effects with sham stimulation.

However, the implementation of active control utilising M1s' hand area yielded no discernible effect on the stimulation regions compared to lateralised TUS of the FEFs. Unlike Kubanek and colleagues (2020), we found no evidence of region-specific bias effects of TUS. This disparity may be attributed to our consecutive blocks of FEF and M1 within a single stimulation session, whereas Kubanekand colleagues employedseparate stimulation sessions for each stimulation region and side, spread across different days, which may have more effectively isolatenull effects for the active control region.

Additionally, our assessment of auditory maskingrevealed that participants tended to believe they could distinguish between sham and TUS, and their perception for stimulation sides differed. This outcome was not aligned with our intention to blind participants to various stimulation conditions. Nonetheless, participants appeared toshow a high tendency to guess they were stimulated when receiving TUS. Furthermore, there was a bias towards believing stimulation occurred on the right side, even when it was delivered on the left. Participants also struggled to accurately discern the specific stimulation conditions and sides, which became evident during the evaluation of theirexperience with TUS. They were required to indicate their beliefs, even when uncertain. This emphasises the importance of considering participants' perception and subjective experiences alongside objective measureswhen evaluating the effects of TUS.

Lastly, our study presents preliminary results from eight participants as part of an ongoing project aiming to collect data from 36 participants, hence the independent effects reported.

Conclusion

As TUS is still in its foundational stage for human use and gainsrecognition as a promisingnon-invasive brainstimulation technique, thereis a critical need to establish an effective online TUS protocol. This protocol should aim to maximise efficacy while minimising confounding factors and gain insights into the neuromodulatory effects. Our preliminary results suggest an excitatory effect induced by TUS of the left FEF effect onsaccadic direction while TUS of the right FEF hints at a potential perturbatory effect on saccadic accuracy. Future research should prioritise robust methodologies that account for inherent characteristics of the stimulation region, inter-individual differences, and peripheral confounding factors, thereby isolating direct neuromodulatory effects of TUS. This endeavour is essential for realising the potential for TUS use in humans in both research and clinical settings.

Supplemental materials

Table S1 *Functional localisers for TUS delivery*

contrast	region of activation		*x* (mm)	*y* (mm)	*z* (mm)	$t_{(288)}$ value	cluster size
follow – fixation	left FEF	Group-level (*N* = 17) MNI coords	**-24 ± 7.11**	**-7 ± 9.50**	**50 ± 12.33**	11.56	27
		Single-subject level	-27	-15	63	25.47	5157
			-24	-21	55	13.68	3778
			-30	-20	33	16.19	609
			-14	-17	51	14.20	3873
			-15	-29	44	15.56	1997
			-28	-13	65	8.21	108
			-23	-17	36	15.08	1156
			-23	-23	55	15.65	877
			-42	-11	34	13.39	1151
			-29	-8	69	18.45	3513
			-28	9	49	13.43	868
			-20	-19	51	8.91	206
			-17	6	47	12.21	4198
			-30	-22	46	17.12	3928
			-24	-37	24	12.02	3167
			-17	-25	58	15.70	5708
			-32	-13	38	12.45	519
follow – fixation	right FEF	Group-level (*N* = 17) MNI coords	**39 ± 4.47**	**-4 ± 10.66**	**47 ± 12.28**	13.53	37
		Single-subject level	22	-9	72	16.82	5157
			20	-24	48	17.12	101190
			19	-21	43	10.19	214
			18	-13	44	11.88	852
			30	-31	37	19.25	1693
			19	-10	63	13.56	958
			31	-17	38	9.63	572
			23	-29	58	9.44	905
			24	-16	42	13.09	1908
			23	-6	70	20.48	3513
			22	-8	47	10.81	571
			32	-16	40	8.81	272
			19	9	49	12.42	4198
			24	-14	49	18.21	3928
			18	-33	23	12.13	316710
			19	-3	44	13.41	5708
			22	-13	43	12.77	792

						$t_{(192)}$ value	
right fingers – left fingers	left M1	Group-level (N = 17) MNI coords	**-36 ± 4.52**	**-22 ± 19.72**	**53 ± 11.69**	11.42	122
		Single-subject level	-35	-33	69	21.08	1210
			-39	-36	44	21.81	1573
			-35	-47	45	16.93	838
			-29	-34	46	15.88	838
			-33	-47	35	29.07	1901
			-42	-29	56	30.32	1606
			-30	-36	43	23.76	1454
			-32	-41	53	20.60	1405
			-39	-31	33	21.15	5996
			-30	-27	64	20.34	1631
			-36	-16	45	14.25	1993
			-32	-31	38	8.91	2119
			-28	-17	57	18.28	1330
			-35	-38	54	25.81	1013
			-34	-49	23	21.28	2382
			-25	-38	40	20.40	2865
			-39	-32	38	36.38	1900
			-38	-36	22	23.07	1209
left fingers – right fingers	right M1	Group-level (N = 17) MNI coords	**36 ± 4.60**	**-19 ± 10.11**	**53 ± 13.46**	12.26	76
		Single-subject level	31	-27	71	24.65	1367
			29	-40	42	2408	1677
			34	-34	43	24.06	1393
			29	-31	43	23.33	1714
			29	-51	36	19.40	1301
			28	-30	64	38.77	5357
			30	-37	42	26.31	1789
			30	-44	55	2316	1341
			29	-33	34	13.20	840
			26	-22	73	18.94	1122
			26	-27	54	20.08	1037
			40	-28	41	27.52	1402
			38	-13	54	16.31	1558
			27	-40	55	19.03	1252
			22	-53	21	12.81	885
			30	-26	44	21.30	3022
			23	-333	40	24.63	2709

Abbreviations: FEF = Frontal Eye Field; M1= primary motor cortex, hand area

Bias effect on saccadicdirection at single-subject level

Methods

We explored the potential bias effect, whether excitatory or inhibitory, at the single-subject level. First, we employed Bayesian Logistic Regression models with theBernoulli family in conjunction with theidentity link, and 10,000 iterations using brms (version 2.16.3;Bürkner, 2017) on the same pre-processed TUS data. The model examined the probability of executing a rightward saccade as a function of target onset delays. Subsequently, model estimates and marginal means of each sigmoid parameter per stimulation condition were computed using emmeans package (version 1.1, Lenth et al., 2018.

Fundamentally, Bayesian statistics views probability as a measure of belief in an event or hypothesis. It employs Bayes' theorem to determine the probability of a hypothesis givenavailable data. In our study,we applied this framework to assess the probability of three sigmoidparameters: bias, sigma,and lapse. Bias, consistent with prior models, indicated the horizontal shift of the probability of rightward fixationat a target delay of 0 milliseconds, potentially reflecting excitatory or inhibitory effects. Sigma represented the slope of the sigmoid curve, reflecting the vertical shift of the sigmoid curve and a possible perturbatory effect. Lapse referredto the horizontal asymptotes at y = 0 and y = 1, indicating the limits or saturation point of the probability of rightward fixation. Initially, we set non-informative priors for each parameter. For bias and sigma, we chose a normal prior distribution with a mean of 0 and a standard deviationof 0.6, with sigma bounded between 0 and 1 to ensure positivity. Lapse was governed by a beta distribution with shape parameters derived from a uniform distribution and bounded between 0 and 0.5. These priors allowed data to inform parameter estimates while imposing necessary constraints, such as non-negativity or limited range.As the model assimilated new data, it updated beliefs by evaluating the likelihood of the data given the hypothesis and applying Bayes' theorem to adjust our beliefs accordingly.

In the Bayesian logistic regression framework, we calculated the Odds Ratio (OR) for each bias partial effect to gauge the strength and direction of association, serving as a measure of effect size. An OR exceeding 1 indicates a positive association, signifying higherodds of the event occurringin one stimulation condition comparedto another. Conversely, an OR below 1 denotes a negative association, indicating lower odds of the event occurring in one stimulation condition compared to another.

After iterating the model 10,000 times, we computed marginal means using emmeans()pairwise and plotted them for the bias parameter per stimulation condition.Our primary focus was on comparing the marginal means of the bias parameter,which represents the average bias—either excitatory or inhibitory—at a target delay of 0 milliseconds per stimulation condition. Conversely, marginal means of sigma cannot effectively capture the slope across a range of short target delays per stimulation conditiondue to averaging, leading to information loss for slope inference. Therefore, we concentrated solely on examining the bias parameter.

For excitatory bias effects, we anticipated that TUS of the left FEF would yield a leftward horizontal shift, while TUS of the right FEF would show a rightward bias, indicating an excitatory bias. Conversely, for inhibitory bias effects, we hypothesised that TUS of the left FEF would show a rightward bias, while TUS of the right FEF would demonstrate leftward bias. Additionally, we expected bilateral TUS of M1s and sham stimulation to have no significant effect on saccadic behaviour, serving as a control for TUS of the FEFs.

Results

We found no conclusive evidence for either excitatory or inhibitory bias for each of the eight participants (referto Table S2 and Figure S1). Interestingly, only sub-008 showeda partial effect, where TUS of the right FEF increasedleftward bias relativeto TUS of the leftFEF, while sham and TUS of M1s served as control (Estimate: 0.03, ES = 0.01, 95% CI [0.01, 0.01], OR = 1.03). This observation supports the excitatory hypothesis. However, it is essentialto note that the OR, which represents the effect size of sub-008's partial effects, was 1.03. Additionally, the control conditions did not clearly demonstrate an unaffected midpoint between TUS of the left and right FEFs for each participant (refer to Table S2), indicating that the suggested excitatory effect cannot be conclusively interpreted at single-subject level.

Table S2 Partial effects for bias per stimulation condition per participant, relative to left FEF TUS

Participant	Effect	*Estimate*	*ES*	95% CI	OR
sub-002	right FEF	0.01	0.01	[-0.01, 0.03]	1.01
	sham	0.02	0.01	[0.01, 0.04] *	1.02
	left M1	0.01	0.01	[-0.00, 0.03]	1.01
	right M1	0.01	0.01	[-0.00, 0.03]	1.01
sub-003	right FEF	0.00	0.01	[-0.01, 0.02]	1.00
	sham	0.00	0.01	[0.01, -0.01]	1.00
	left M1	-0.00	0.01	[0.01, -0.02]	1.00
	right M1	0.01	0.01	[0.01, -0.00]	1.01
sub-004	right FEF	0.01	0.01	[-0.01, 0.03]	1.01
	sham	-0.00	0.01	[-0.02, 0.02]	1.00
	left M1	-0.00	0.01	[-0.02, 0.02]	1.00
	right M1	-0.01	0.01	[-0.03, 0.01]	1.01
sub-005	right FEF	0.01	0.01	[-0.02, 0.00]	1.01
	sham	0.01	0.01	[-0.01, 0.02]	1.01
	left M1	-0.01	0.01	[-0.02, 0.01]	1.01
	right M1	0.02	0.01	[0.00, 0.03] *	
sub-006	right FEF	0.01	0.01	[-0.02, -0.00]	1.01
	sham	0.01	0.01	[-0.01, 0.02]	1.01
	left M1	-0.00	0.01	[-0.02, 0.01]	1.00
	right M1	-0.00	0.01	[-0.01, 0.01]	1.00
sub-007	right FEF	0.00	0.01	[-0.01, 0.02]	1.00
	sham	0.01	0.01	[-0.01, 0.02]	1.01
	left M1	0.00	0.01	[-0.01, 0.02]	1.00
	right M1	0.02	0.01	[0.01, 0.00] *	1.02
sub-008	right FEF	0.03	0.01	[0.01, 0.01] *	1.03
	sham	0.01	0.01	[0.01, -0.01]	1.01
	left M1	0.01	0.01	[-0.00, 0.03]	1.01
	right M1	0.01	0.01	[0.01, -0.01]	1.01
sub-011	right FEF	-0.00	0.01	[-0.02, 0.01]	1.00
	sham	-0.00	0.01	[-0.02, 0.01]	1.00
	left M1	-0.00	0.01	[-0.02, 0.01]	1.00
	right M1	0.01	0.01	[-0.01, 0.02]	1.01

* indicates bias effect of given stimulation condition is significantly different from 0 with $p = .05$
Abbreviations: ES = Estimated Error; CI = Credible Interval, OR = Odds Ratio

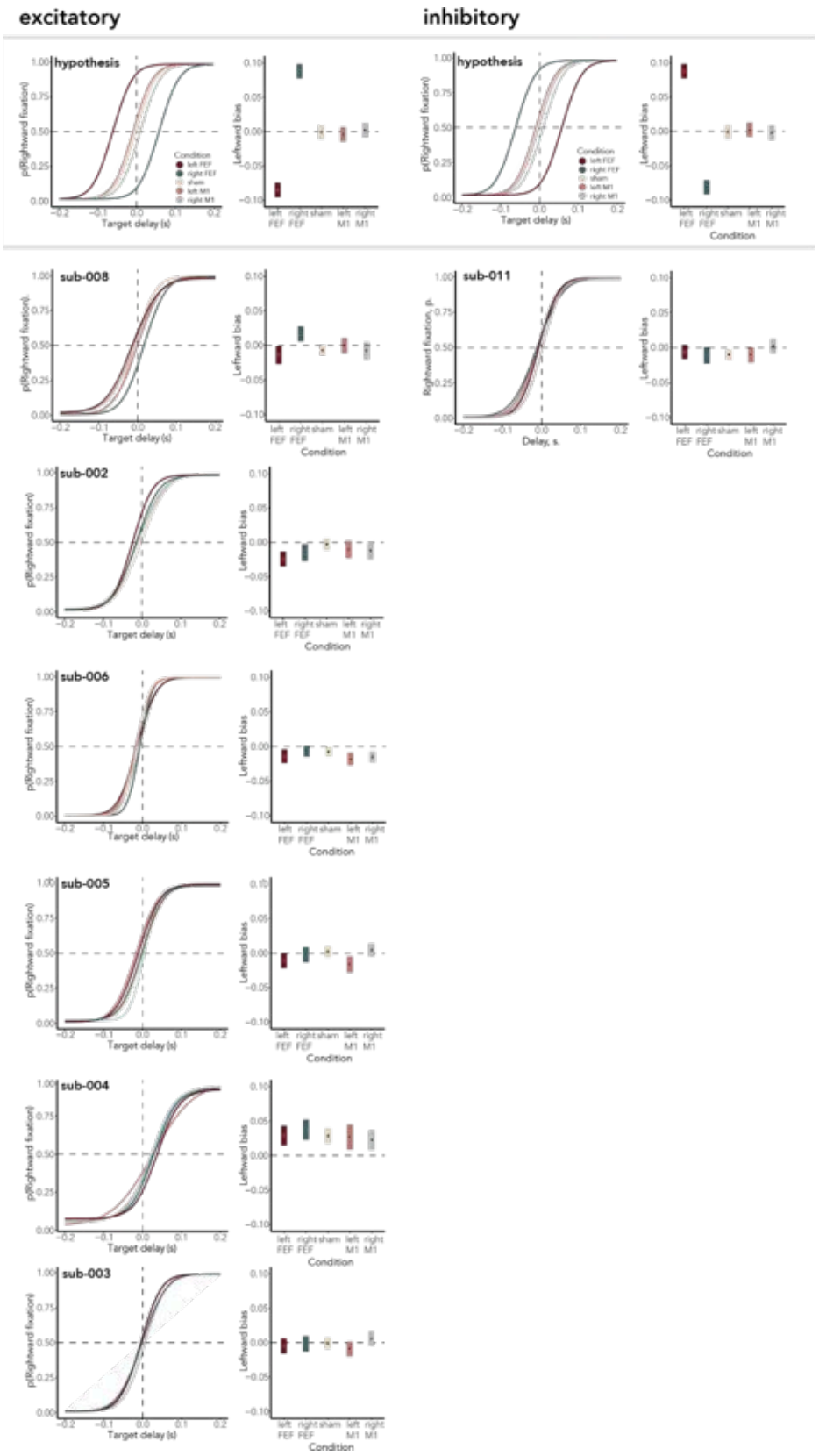

Figure S1 | Sigmoid curves and marginal means for bias parameter depict probability of executing a rightward saccade as a function of target onset delays per stimulation condition per participant.

Baseline GABA level

Methods

We quantified GABA concentrations in institutional units (IU) withinthe left FEF and M1 regions (N = 5; three participants were excluded due to model fit issues) using the Gannet MATLAB-based toolkit (Edden et al., 2014). This involved a series of steps including preprocessing, spectral processing, quantification,analysis, and qualitycontrol. Employing Pearson'scorrelation, we assessedthe relationship betweenGABA concentrations and the random intercept for the saccadicaccuracy effect inducedby TUS on the FEFs. The extent of TUS effect on saccadic accuracy served as the dependentvariable, where a lower value indicates a stronger perturbatory effect and, therefore, a higher susceptibility to TUS neuromodulation. A positive correlation between accuracy effectsof TUS of the FEFs and baselineGABA levels would suggest a lesser perturbatory effect of FEF TUS associated with higher baseline GABA levels, while a negative correlation would imply a stronger perturbatory effect of TUS of the FEFs related to decreaesd baseline GABA levels, of which the latter impliesan increased susceptibility to neuromodulation with decreased ratio of an inhibitory neurotransmitter.

Results

Pearson's correlation analysis showed no significant correlation between the extent of perturbatory effect on saccadic accuracy and baseline level of GABA in the left FEF ($r(3) = -0.39$, $p = .72$, Figure S2A). Similarly, no correlation was found betweensaccadic accuracy perturbation and baseline GABA levels in M1 ($r(3) = 0.16$, $p = .88$, Figure S2B). These results suggest that the baseline level of GABA may not play a significant role in susceptibility to neuromodulation. However, given the small sample size, these correlations should be interpreted cautiously.

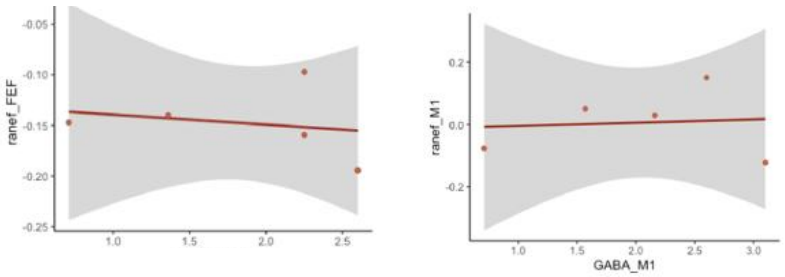

FigureS2 | TUS effect on saccadic accuracyas a function of baselineGABA level . (A) GABA baseline concentration within left FEF shows no clear effect on the extent of TUS on FEFS effect on saccadic accuracy. Note high variance of two correlations towards higher concentrations of GABA baseline, (B) GABA baseline concentration within left M1 yields no association with the extent of TUS of FEFs effect on saccadicaccuracy.

References

Amiez, C., Kostopoulos, P., Champod, A.-S., & Petrides, M. (2006). Local morphology predicts functional organization of the dorsal premotor region in the human brain. The Journal of Neuroscience, 26(10), 2724–2731. https://doi.org/10.1523/JNEUROSCI.4739-05.2006

Amiez, C., & Petrides, M. (2009). Anatomical organization of the eye fields in the human and non-human primate frontal cortex. Progress in neurobiology, 89(2), 220-230. https://doi.org/10.1016/j.pneurobio.2009.07.010

Barr, D. J., Levy, R., Scheepers, C., & Tily, H. J. (2013). Random effects structure for confirmatory hypothesis testing: Keep it maximal. Journal of memory and language, 68(3), 255-278. https://doi.org/10.1016/j.jml.2012.11.001

Bates, D., Maechler, M., Bolker, B., & Walker, S. (2015). Fitting linear mixed-effects model using lme4. Journal of Statistical Software, 67(1), 1-48. doi:10.18637/jss.v067.i01.

Butler, C. R., Rhodes, E., Blackmore, J., Cheng, X., Peach, R. L., Veldsman, M., Sheerin, F., &

Cleveland, R. O. (2022). Transcranial ultrasound stimulation to human middle temporal complex improves visual motion detection and modulates electrophysiological responses. Brain Stimulation, 15(5), 1236-1245. https://doi.org/10.1016/j.brs.2022.08.022

Beurze, S. M., de Lange, F. P., Toni, I., & Medendorp, W. P. (2009). Spatial and effector processing in the human parietofrontal network for reaches and saccades. Journal of neurophysiology, 101(6), 3053–3062. https://doi.org/10.1152/jn.91194.2008

Brown, M. R., Vilis, T., & Everling, S. (2007). Frontoparietal activation with preparation for antisaccades. Journal of Neurophysiology, 98(3), 1751-1762. https://doi.org/10.1152/jn.00460.2007

Cameron, I. G., Riddle, J. M., & D'Esposito, M. (2015). Dissociable roles of dorsolateral prefrontal cortex and frontal eye fields during saccadic eye movements. Frontiers in human neuroscience, 9, 613. https://doi.org/10.3389/fnhum.2015.00613

Curtis, C. E. (2006). Prefrontal and parietal contributions to spatial working memory. Neuroscience, 139(1),173-180. https://doi.org/10.1016/j.neuroscience.2005.04.070

Curtis, C. E., & D'Esposito, M. (2006). Selection and maintenance of saccade goals in the human frontal eye fields. Journal of Neurophysiology, 95(6), 3923-3927. https://doi.org/10.1152/jn.01120.2005

Curtis, C. E., & Connolly, J. D. (2008). Saccade preparation signals in the human frontal and parietal cortices. Journal of Neurophysiology, 99(1), 133-145. https://doi.org/10.1152/jn.00899.2007

Curtis, C. E., & Connolly, J. D. (2008). Saccade preparation signals in the human frontal and parietal cortices. Journal of Neurophysiology, 99(1), 133-145. https://doi.org/10.1152/jn.00899.2007

Darmani, G., Bergmann, T. O., Butts Pauly, K., Caskey, C. F., de Lecea, L., Fomenko, A., Fouragnan, E., Legon, W., Murphy, K. R., Nandi, T., Phipps, M. A., Pinton, G., Ramezanpour, H., Sallet, J., Yaakub, S. N., Yoo, S. S., & Chen, R. (2022). Non-invasive transcranial ultrasound stimulation for neuromodulation. Clinical Neurophysiology, 135, 51–73. https://doi.org/10.1016/j.clinph.2021.12.010

Farboud, S., Walstra, S. L. Y., Chetverikov, A., Kop, B., Marques, J. P., Verhagen, L., & den Ouden, H. E. (2023). Biasing choice through transcranial ultrasonic stimulation of the frontal eye fields in humans. https://doi.org/10.17605/OSF.IO/K5P2M

Faul, F., Erdfelder, E., Buchner, A., & Lang, A.-G. (2009). Statistical power analyses using G*Power 3.1: Tests for correlation and regression analyses. Behavior Research Methods, 41, 1149-1160. https://doi.org/10.3758/BRM.41.4.1149

Folloni, D., Fouragnan, E., Wittmann, M. K., Roumazeilles, L., Tankelevitch, L., Verhagen, L., Attali, D., Aubry, J.F., Sallet, J., & Rushworth, M. F. (2021). Ultrasound modulation of macaque prefrontal cortex selectively alters credit assignment–related activity and behavior. Science Advances, 7(51). https://doi.org/10.1126/sciadv.abg7700

Folloni, D., Verhagen, L., Mars, R. B., Fouragnan, E., Constans, C., Aubry, J.-F., Rushworth, M. F. S., & Sallet, J. (2019). manipulation of subcortical and deep cortical activity in the primate brain using transcranial focused ultrasound stimulation. Neuron, 101(6), 1109-1116.e5. https://doi.org/10.1016/j.neuron.2019.01.019

Fouragnan, E. F., Chau, B. K. H., Folloni, D., Kolling, N., Verhagen, L., Klein-Flügge, M., Tankelevitch, L., Papageorgiou, G. K., Aubry, J. F., Sallet, J., & Rushworth, M. F. S. (2019). The macaque anterior cingulate cortex translates counterfactual choice value into actual behavioral change. Nature neuroscience, 22(5), 797–808. https://doi.org/10.1038/s41593-019-0375-6

Gagnon, D., O'Driscoll, G. A., Petrides, M., & Pike, G. B. (2002). The effect of spatial and temporal information on saccades and neural activity in oculomotor structures. Brain, 125(1), 123-139. https://doi.org/10.1093/brain/awf005

Grosbras M. H., Paus T. (2002). Transcranial magnetic stimulation of the human frontal eye field: effects on visual perception and attention. Journal of Cognitive Neuroscience, 14 (1109-1120). https://doi.org/10.1162/089892902320474553

Grosbras, M. H., & Paus, T. (2003). Transcranial magnetic stimulation of the human frontal eye field facilitates visual awareness. European Journal of Neuroscience, 18(11), 3121-3126. https://doi.org/10.1111/j.1460-9568.2003.03055.x

Halekoh, U., & Højsgaard, S. (2014). A Kenward-Roger approximation and parametric bootstrap methods for tests in linear mixed models -- the {r}package {pbkrtest} (R package version 0.5.1) [Computer software]. The Comprehensive R Archive Network. https://www.jstatsoft.org/v59/i09/

Hung, J., Driver, J., & Walsh, V. (2011). Visual selection and the human frontal eye fields: effects of frontal transcranial magnetic stimulation on partial report analyzed by Bundesen's theory of visual attention. Journal of Neuroscience, 31(44), 15904-15913. https://doi.org/10.1523/JNEUROSCI.2626-11.2011

Hutchison, R. M., Gallivan, J. P., Culham, J. C., Gati, J. S., Menon, R. S., & Everling, S. (2012). Functional connectivity of the frontal eye fields in humans and macaque monkeys investigated with resting-state fMRI. Journal of neurophysiology, 107(9), 2463-2474. https://doi.org/10.1152/jn.00891.2011

Ioannides, A. A., Fenwick, P. B., Pitri, E., & Liu, L. (2010, June). A step towards non-invasive characterization of the human frontal eye fields of individual subjects. In Nonlinear Biomedical Physics 4(1), 1-10. https://doi.org/10.1186/1753-4631-4-S1-S11

Jerusalem, A., Al-Rekabi, Z., Chen, H., Ercole, A., Malboubi, M., Tamayo-Elizalde, M., Verhagen, L., & Contera, S. (2019). Electrophysiological-mechanical coupling in the neuronal membrane and its role in ultrasound neuromodulation and general anaesthesia. Acta biomaterialia, 97, 116-140. https://doi.org/10.1016/j.actbio.2019.07.041

Kop, B. R., Shamli Oghli, Y., Grippe, T. C., Nandi, T., Lefkes, J., Meijer, S. W., Farboud, S., Engels, M., Hamani, M., Null, M., Radetz, A., Hassan, U., Darmani, G., Chetverikov, A., den Ouden, H. E. M., Bergmann, T.O., Chen, R., & Verhagen, L. (2023). Auditory confounds can drive online effects of transcranial ultrasonic stimulation in humans. bioRxiv, 2023-02 https://doi.org/10.1101/2023.02.22.527901

Kop, B. R., Shamli Oghli, Y., Grippe, T. C., Nandi, T., Lefkes, J., Meijer, S. W., Farboud, S., Engels, M., Hamani, M., Null, M., Radetz, A., Hassan, U., Darmani, G., Chetverikov, A., den Ouden, H. E. M., Bergmann, T.O., Chen, R., & Verhagen, L. (2023). Auditory confounds can drive online effects of transcranial ultrasonic stimulation in humans. bioRxiv, 2023-02. https://doi.org/10.1101/2023.02.22.527901

Khalighinejad, N., Priestley, L., Jbabdi, S., & Rushworth, M. F. (2020). Human decisions about when to act originate within a basal forebrain–nigral circuit. Proceedings of the National Academy of Sciences, 117(21), 11799-11810. https://doi.org/10.1073/pnas.1921211117

Kubanek, J., Brown, J., Ye, P., Pauly, K. B., Moore, T., & Newsome, W. (2020). Remote, brain region-specific control of choice behavior with ultrasonic waves. Science Advances, 6(21), eaaz4193. https://doi.org/10.1126/sciadv.aaz4193

Murd, C., Moisa, M., Grueschow, M. Polania, R., & Ruff, C. C. (2020). Causal contributions of human frontal eye fields to distinct aspects of decision formation. Scientific Reports 10, 7317 (2020). https://doi.org/10.1038/s41598-020-64064-7

Nakajima, K., Osada, T., Ogawa, A., Tanaka, M., Oka, S., Kamagata, K., Aoki, S., Oshima, Y., Tanaka, S., & Konishi, S. (2022). A causal role of anterior prefrontal-putamen circuit for response inhibition revealed by transcranial ultrasound stimulation in humans. Cell Reports, 40(7). https://doi.org/10.1016/j.celrep.2022.111197

Neggers, S. F., Van Diepen, R. M., Zandbelt, B. B., Vink, M., Mandl, R. C., & Gutteling, T. P. (2012). A functional and structural investigation of the human fronto-basal volitional saccade network. PLoS One, 7(1), e29517. https://doi.org/10.1371/journal.pone.0029517

Paus, T. (1996). Location and function of the human frontal eye-field: a selective review. Neuropsychologia, 34(6), 475-483. https://doi.org/10.1016/0028-3932(95)00134-4

Petrides, M., Tomaiuolo, F., Yeterian, E. H., & Pandya, D. N. (2012). The prefrontal cortex: comparative architectonic organization in the human and the macaque monkey brains. cortex, 48(1), 46-57. https://doi.org/10.1016/j.cortex.2011.07.002

Preuss, T. M., & Goldman-Rakic, P. S. (1991). Myelo-and cytoarchitecture of the granular frontal cortex and surrounding regions in the strepsirhine primate Galago and the anthropoid primate Macaca. Journal of Comparative Neurology, 310(4), 429-474. https://doi.org/10.1002/cne.903100402

R Core Team (2021). R: A language and environment for statistical computing [Computer software]. The Comprehensive R Archive Network. https://www.R-project.org/

RStudio Team. (2021). RStudio: Integrated development environment for R. [Computer software]. Boston, MA. http://www.rstudio.com/

Revelle (2023). psych: Procedures for Psychological, Psychometric, and Personality Research. Northwestern University, Evanston, Illinois. R package version 2.3.6, https://CRAN.R-project.org/package=psych.

Reznik, S. J., Sanguinetti, J. L., Tyler, W. J., Daft, C., & Allen, J. J. (2020). A double-blind pilot study of transcranial ultrasound (TUS) as a five-day intervention: TUS mitigates worry among depressed participants. Neurology, Psychiatry and Brain Research, 37, 60-66. https://doi.org/10.1016/j.npbr.2020.06.004

Schlag, J., Dassonville, P., & Schlag-Rey, M. (1998). Interaction of the two frontal eye fields before saccade onset. Journal of Neurophysiology, 79(1), 64-72. https://doi.org/10.1152/jn.1998.79.1.64

Sorum, B., Rietmeijer, R. A., Gopakumar, K., Adesnik, H., & Brohawn, S. G. (2021). Ultrasound activates mechanosensitive TRAAK K+ channels through the lipid membrane. Proceedings of the National Academy of Sciences, 118(6), e2006980118. https://doi.org/10.1073/pnas.2006980118

Sorum, B., Rietmeijer, R. A., Gopakumar, K., Adesnik, H., & Brohawn, S. G. (2021). Ultrasound activates mechanosensitive TRAAK K+ channels through the lipid membrane. Proceedings of the National Academy of Sciences, 118(6), e2006980118. https://doi.org/10.1073/pnas.2006980118

Stanton, G. B., Deng, S. Y., Goldberg, E. M., & McMullen, N. T. (1989). Cytoarchitectural characteristic of the frontal eye fields in macaque monkeys. Journal of Comparative Neurology, 282(3), 415-427. https://doi.org/10.1002/cne.902820308

Tzourio-Mazoyer, N., Petit, L., Zago, L., Crivello, F., Vinuesa, N., Joliot, M., Jobard, G., Mellet, E., & Mazoyer, B. (2015). Between-hand difference in ipsilateral deactivation is associated with hand lateralization: fMRI mapping of 284 volunteers balanced for handedness. Frontiers in Human Neuroscience, 9, 5. https://doi.org/10.3389/fnhum.2015.00005

Verhagen, L., Gallea, C., Folloni, D., Constans, C., Jensen, D. E., Ahnine, H., Roumazeilles, L., Santin, M., Ahmed, B., Lehericy, S., Klein-Flügge, M. C., Krug, K., Mars, R. B., Rushworth, M. F., Pouget, P., Aubry, J.-F., & Sallet, J. (2019). Offline impact of transcranial focused ultrasound on cortical activation in primates. ELife, 8, e40541. https://doi.org/10.7554/eLife.40541

Vernet, M., Quentin, R., Chanes, L., Mitsumasu, A., & Valero-Cabré, A. (2014). Frontal eye field, where art thou? Anatomy, function, and non-invasive manipulation of frontal regions involved in eye movements and associated cognitive operations. Frontiers in Integrative Neuroscience, 8, 66. https://doi.org/10.3389/fnint.2014.00066

Wattiez, N., Constans, C., Deffieux, T., Daye, P. M., Tanter, M., Aubry, J. F., & Pouget, P. (2017). Transcranial ultrasonic stimulation modulates single-neuron discharge in macaques performing an antisaccade task. Brain stimulation, 10(6), 1024-1031. https://doi.org/10.1016/j.brs.2017.07.007

Yaakub, S. N., White, T. A., Roberts, J., Verhagen, L., Stagg, C. J., Hall, S. D., & Fouragnan, E. F. (2023). Transcranial focused ultrasound-mediated neurochemical and functional connectivity changes in deep cortical regions in humans. bioRxiv, 2023-01. https://doi.org/10.1101/2023.01.20.524869

Yang, P. S., Kim, H., Lee, W., Bohlke, M., Park, S., Maher, T. J., & Yoo, S. S. (2012). Transcranial focused ultrasound to the thalamus is associated with reduced extracellular GABA levels in rats. Neuropsychobiology, 65(3), 153–160. https://doi.org/10.1159/000336001

Yoo, S., Mittelstein, D. R., Hurt, R. C., Lacroix, J., & Shapiro, M. G. (2022). Focused ultrasound excites cortical neurons via mechanosensitive calcium accumulation and ion channel amplification. Nature communications, 13(1), 493. https://doi.org/10.1038/s41467-022-28040-1

Zhu, J., Xian, Q., Hou, X., Wong, K. F., Zhu, T., Chen, Z., He, D., Kala, S., Murugappan, S., Jing, J., Wu, Y., Li, D., Guo, J., Qiu, Z., & Sun, L. (2023). The mechanosensitive ion channel Piezo1 contributes to ultrasound neuromodulation. Proceedings of the National Academy of Sciences, 120(18), e2300291120. https://doi.org/10.1073/pnas.2300291120